Journal of Nanobiotechnology

REVIEW

Open Access

Electrochemical aptasensor based on the engineered core-shell MOF nanostructures for the detection of tumor antigens

Suliman Khan[1,2], William C. Cho[3], Afrooz Sepahvand[4], Sara Haji Hosseinali[5], Arif Hussain[6], Mohammad Mahdi Nejadi Babadaei[7], Majid Sharifi[8,9], Mojtaba Falahati[10,11*], Laila Abdulmohsen Jaragh-Alhadad[12*], Timo L. M. ten Hagen[10,11*] and Xin Li[13*]

Abstract

It is essential to develop ultrasensitive biosensors for cancer detection and treatment monitoring. In the development of sensing platforms, metal-organic frameworks (MOFs) have received considerable attention as potential porous crystalline nanostructures. Core-shell MOF nanoparticles (NPs) have shown different diversities, complexities, and biological functionalities, as well as significant electrochemical (EC) properties and potential bio-affinity to aptamers. As a result, the developed core-shell MOF-based aptasensors serve as highly sensitive platforms for sensing cancer biomarkers with an extremely low limit of detection (LOD). This paper aimed to provide an overview of different strategies for improving selectivity, sensitivity, and signal strength of MOF nanostructures. Then, aptamers and aptamers-modified core-shell MOFs were reviewed to address their functionalization and application in biosensing platforms. Additionally, the application of core-shell MOF-assisted EC aptasensors for detection of several tumor antigens such as prostate-specific antigen (PSA), carbohydrate antigen 15-3 (CA15-3), carcinoembryonic antigen (CEA), human epidermal growth factor receptor-2 (HER2), cancer antigen 125 (CA-125), cytokeratin 19 fragment (CYFRA21-1), and

*Correspondence:
Mojtaba Falahati
m.falahati@erasmusmc.nl
Laila Abdulmohsen Jaragh-Alhadad
Laila.alhadad@ku.edu.kw
Timo L. M. ten Hagen
t.l.m.tenhagen@erasmusmc.nl
Xin Li
lizn99999@163.com
[1] Medical Research Center, The Second Affiliated Hospital of Zhengzhou University, Zhengzhou, China
[2] Department of Medical Lab Technology, The University of Haripur, Haripur, Pakistan
[3] Department of Clinical Oncology, Queen Elizabeth Hospital, Kowloon, Hong Kong, China
[4] Department of Cellular and Molecular Biology, Faculty of Advanced Science and Technology, Tehran Medical Sciences, Islamic Azad University, Tehran, Iran
[5] Department of Genetics, Faculty of Advanced Science and Technology, Tehran Medical Sciences, Islamic Azad University, Tehran, Iran
[6] School of Life Sciences, Manipal Academy of Higher Education, Dubai, United Arab Emirates
[7] Department of Molecular Genetics, Faculty of Biological Science, North Tehran Branch, Islamic Azad University, Tehran, Iran
[8] Student Research Committee, School of Medicine, Shahroud University of Medical Sciences, Shahroud, Iran
[9] Depatment of Tissue Engineering, School of Medicine, Shahroud University of Medical Sciences, Shahroud, Iran
[10] Precision Medicine in Oncology (PrMiO), Department of Pathology, Erasmus MC Cancer Institute, Erasmus MC, Rotterdam, The Netherlands
[11] Nanomedicine Innovation Center Erasmus (NICE), Erasmus MC, Rotterdam, The Netherlands
[12] Department of Chemistry, College of Science, Kuwait University, 13060 Safat, Kuwait
[13] Department of Neurology, The Second Affiliated Hospital of Zhengzhou University, Zhengzhou, China

other tumor markers were discussed. In conclusion, the present article reviews the advancement of potential biosensing platforms toward the detection of specific cancer biomarkers through the development of core-shell MOFs-based EC aptasensors.

Keywords Core-shell, Metal organic framework, Aptasensors, Cancer biomarkers

Introduction

Biomarker detection plays a major role in the timely diagnosis of a wide range of disorders, including neurodegenerative, autoimmune and cancer diseases. The discovery of cancer biomarkers may lead to the early detection of cancer, which in turn will significantly impact reducing cancer-related mortality. Also, monitoring the treatment process, diagnosis, and application of an appropriate strategy for cancer therapy, assessment of disease status, drug production, and prescription of appropriate drugs can be done with the help of biomarkers.

As a result, biomedical researchers are increasingly focused on developing a feasible and accurate approach that will result in the sensitive detection of biomarkers. Currently, multiple analytical analyses have been applied for detecting cancer-related biomarkers including spectrophotometry [1, 2], electrophoresis [3, 4], liquid chromatography [5, 6], and sensor [7–9]. For example, surface-enhanced Raman spectroscopy nanoprobes have been widely used for the detection of cancer cells [10], exosomes [11, 12], and protein biomarkers [13].

Furthermore, two-dimensional differential gel electrophoresis has been demonstrated as a promising platform for the detection of various types of cancer biomarkers with high reproducibility and sensitivity [14]. Furthermore, liquid chromatography coupled to mass spectrometry has been broadly utilized for the potential detection of cancer biomarker peptides [15], plasma lipid profile [16], splicing biomarkers [17], and modified nucleosides [18]. Also, different types of biosensors including EC-, optical-, and mass-based techniques have been used to detect cancer biomarkers [7, 19, 20]. EC-based biosensing assays stand out among different types of analytical methods and biosensors due to their fast reactivity, high sensitivity, easy operation, and cost-effectiveness. In the recent years, different types of nanomaterials including iron oxide NP bioconjugates [21], gold (Au) NP decorated multiwall carbon nanotubes- [22], sandwiched silver (Ag) NPs in N-doped graphene- [23], AuNPs/graphene quantum dots (QDs)/graphene oxide (GO) film- [24], and hierarchical flower-like molybdenum disulphide (MoS_2) NP- [25] modified EC electrodes have been used to detect cancer biomarkers. However, some major drawbacks including narrow linear range and limited sensitivity still hinder their potential application in the biomedical field. Hence, it is inevitable to develop new electrocatalysts with high sensitivity and selectivity for the detection of cancer biomarkers.

Nonenzymatic-based biosensing approaches show several advantages in comparison with enzymatic-based biosensing strategies including a lower LOD, faster reactive times, improved long/short-term stability, and cost-effectiveness [26–28]. One of the most important strategies for promoting EC detection activity relies on the application of potential materials presenting high conductivity along with a large reactive surface area.

Following the introduction of metal-organic framework (MOF) with 3D periodic infinite network architectures fabricated through the coordination of metals and organic materials as ligands [29, 30], a large number of studies have been published on the synthesis and utilization of colloidal-sized MOF nanostructures [31–33]. In comparison to zeolite- and carbon-based materials, MOF NPs as porous materials exhibit several novel superiorities such as tunable pore dimensions, functionalized pore surfaces, ultralow density, and ultrahigh active surface areas [34], which endow MOFs with exclusive benefits in different applications, including biosensing [35, 36] and catalyst [37, 38]. Recently, there has been a lot of interest in using MOF NPs to develop potential biosensors for the detection of different biological or chemical reactions [39, 40].

Several MOF-based architectures, including nanowires, nanotubes, octahedral, and core-shell structures have been reported for application in different fields [41–43]. Among these structures, core-shell architectures have demonstrated significant advantages due to their highly appealing topologies and potential chemical activities [34]. In comparison to other MOF structures, the presence of a shell can result in the formation of a proportionally stable and unaffected microenvironment for catalytic reactions, as well as the combination of multiple properties via the synergistic feature between the core and shell units [34]. The primary core-shell MOF architectures are identified by a metal core covered with an MOF shell [44]. Nevertheless, there are several common core-shell structures, including metal and nonmetal NPs@MOFs, MOF@metal oxide NPs, and MOFs@MOFs [34, 45, 46].

As a result, because several materials exhibit synergistic performance, the combination of different bio-functional compounds has been a hot topic in the biomedical field. Because of the unique architecture of core-shell MOFs, the developed electrodes exhibit promising long-term stability with boosted mechanical durability [47] and ultra-sensitive EC detection [48]. In fact, core-shell MOFs are used in a variety of biosensors with different detection methods, and have the advantages of exhibiting a rapid reactivity and reusability, as well as improved sensitivity, increased selectivity, and a feasible assay strategy [49, 50].

To date, electrochemistry-based immune assays have been reported for detecting tumor markers with a potential sensitivity and accuracy, a significantly low LOD, and a pronounced signal augmentation [51]. Although this immunoassay has high sensitivity and efficiency, the need for complicated washing steps and heterogeneous responses in this assay cause diverse antibody (Ab)-antigen interactions and diminished Ab performance [52, 53], which affect detection sensitivity and experimental reusability [53]. Aptamers, on the other hand, have different significant advantages over antibodies, including their small size, low cost, increased chemical stability, and feasible design [54, 55]. These characteristics have received widespread attention and have shown promise in addressing the aforementioned immunoassay concerns [56]. Aptamers have also demonstrated some benefits for developing potential biosensors with improved selectivity and sensitivity [57–59].

Therefore, developing potential core-shell MOF with unique structures and recruiting them as a solid support for the immobilization of aptamers can be used to detect different cancer markers. Indeed, when aptamer strands adsorbed onto the MOF platform interact with cancer biomarkers, the resulting conformational changes in the aptamer can be detected using various sensors, particularly EC-based platforms. Additionally, various MOF architectures result in different surface and chemical capabilities, changing the sensing potency of aptamers by regulating the interaction of redox ions with the electrode surface.

Application of core-shell MOFs in the development of biosensing platforms

The application of core-shell MOFs in the development of biosensing platforms is increasing due to their unique functional and structural properties [60]. However, due to the use of the organic ligands and metal ion clusters in the fabrication of these structures, constructing a cohesive and controllable structure remains challenging. In order to overcome some drawbacks such as fine adjustment of the shell thickness, non-uniform growth of the shell, uniform distribution of NPs, reducing the toxicity of reagents, and commercialization by reducing synthesis steps, various methods have been developed to synthesize MOFs. Since different parameters such as temperature, reaction time, pressure, pH, and solvent all have a significant effect on chemical reactions for the synthesis of core-shell MOFs, reproducibility of synthesis parameters is a need for standardization [61, 62]. The most important and common production approaches to synthesize core-shell MOF nanostructure are one-pot synthesis, in situ synthesis, self-assembly, and templating. For further information regarding the synthesis of core-shell MOF nanostructures, the readers shall refer to [34, 46].

Strategies to improve core-shell MOF performance

The very high surface area and porosity of MOFs combined with the multifunctional catalytic activities of metal compounds, have made these materials very susceptible to use in diagnostic platforms. Therefore, to increase the achievement of efficient electron transfer in core-shell MOF-based EC sensors, it is necessary to pay more attention to the selectivity, sensitivity, and reproducibility of MOFs to modulate the LOD and signal amplification.

Enhancement of selectivity

Although surface modification of MOFs is a potential approach in the development of biosensors with high sensitivity and selectivity, structural optimization during the manufacturing process can contribute to improved biosensing capabilities. MOFs with tunable porous structures can be used for the potential detection of biomolecules by developing pore sizes larger than that of the biomolecules. Therefore, by designing MOFs that (1) have pores larger than the size of the biomolecules, such as heterogeneous shell-core structures, or (2) have structural defects in the shell, such as porosities due to oxygen modulation, we can significantly improve the detection range of analysts. In this regard, Yang and coworkers [63] using Cu_xO NPs@ZIF-8 containing pores with controlled dimensions on the shell, were able to detect H_2O_2 molecules with high efficiency and selectivity. This high selectivity was achieved even in the presence of amino acids and biological compounds, whereas metal NPs had low selectivity. Also, Luo and coworkers [64] by creating structural defects in the shell of CeO_2-x/C nanorod with vacancies caused by oxygen modulation and increasing Ce^{3+} ion as a catalytic active site, developed a platform for indirect determination of uric acid at very low working potentials in the presence of high concentration of glucose.

Enhancement of sensitivity

It is well-known that decreasing the size of particles from microparticles to nanomaterials increases the sensitivity of EC sensors/biosensors. In this regard, it has been reported that nano-sized MOFs, when compared to micro-sized MOFs, increase the accessibility of electroactive sites and improve electron transport ability due to increased accessible surface area and higher porosity [65]. In addition, Lopa and coworkers [66] showed that a nano-sized metal azolate framework on the glassy carbon electrode through non-enzymatic detection significantly detected glucose in the dynamic range of 2 to 50 μM and 100 to 1800 μM with a LOD of 0.6 μM compared to bulk MOFs with a LOD of 1.46 μM [67]. In this field, it was recently determined that nano-sized urate oxidase-loaded MOF/boron nanosheets on carbon-glass electrodes improved the LOD of uric acid in the concentration range of 0.1 to 200 μM to 0.025 μM compared to other common electrodes [68]. Nonetheless, it appears that the densely adsorption of MOFs on the electrodes reduces the number of active sites and the corresponding sensor's overall sensitivity. Hence, in order to effectively increase the sensitivity of the biosensors, it is recommended to load a single layer of MOFs on the electrodes [69]. Aside from nano-dimensions, the presence of interconnected pores can improve sensor sensitivity by facilitating electron transfer in the electrodes. For this purpose, it is necessary to investigate the chemical interactions of ligands, their exchange and mixing to create interconnected mesoporous MOFs. For example, Wang and coworkers [70] designed highly interconnected porous Cu-MOFs using an evaporation-based heteroepitaxy and self-assembly process. In this method, after the deposition of copper nanowires on paper through evaporation of dichloromethane-containing nanowires, the paper was immersed in ligand solutions and heteroepitaxial growth was induced to form Cu-MOF crystals. Their results showed that the detection sensitivity of glucose (35.9 $\mu A/cm^2/mm$) and lactate (1690 $\mu A/cm^2/mm$) increases significantly. However, due to the challenge of weak conductivity caused by chemical ligands and inappropriate aggregation of MOFs, the use of nano-hybrids could be a potential approach to increase the sensitivity of biosensors. In addition to increasing catalytic capabilities, nanohybrids can cause enhanced electron transfer in the developed structure. In this regard, it was reported that the electrode engineered with ultra-thin 2D MOF M-TCPP (M = Cu, Co and Ni) nanofilms (1–3 nm) and 2D MOF nanosheets with a thickness of 6–10 nm along with carbon nanosheets obtained from CNT and GO can effectively detect H_2O_2 with improved LOD (5 nM) at the linear range of 0.01–3.75 μM and 3.75–377.75 μM compared to 2D MOF M-TCPP [71]. Recently, in order to increase the LOD of cancer cells by sensing the generated H_2O_2, Huang and coworkers [72] by designing ultra-thin 2D MOF nanosheets based on hybridizing copper nanozymes with Au nanozymes in a non-aggregative form with dual enzyme-like activity were able to remarkably improve the detection of colon cancer cells. They showed that the structural changes induced through the hybridization of Cu nanozymes with Au can improve the LOD of H_2O_2 up to 5.6 nM with a high sensitivity of 188.1 $\mu A/cm^2/mM$ [72]. It was also found that changing the morphology of 2D Zn-MOFs hybridized with Ag NPs stimulated greater electrocatalytic activity for H_2O_2 detection compared to the 3D state [73]. Since Ag/2D Zn-MOFs were able to provide a large surface area and well-dispersion of NPs in their structure, they provide greater electrical conductivity compared to Ag/3D Zn-MOFs. Under optimal conditions, electrodes fabricated with Ag/2D Zn-MOF improved the LOD of H_2O_2 to1.67 μM with a wide range of 5.0 μM to 70 mM [73].

Enhancement of signal strength

The strategy of signal amplification is one of the vital approaches in improving the performance of sensors due to the very low concentration of analytes in biological samples. Despite different strategies in electric signal amplification, the use of molecular biological technologies, enzymatic methods and nanohybrids have received much attention.

One of the signal amplification strategies is the use of molecular biological technologies such as rolling circle amplification, strand displacement amplification, hybridization chain reaction (HCR), and catalytic hairpin assembly. For instance, Chen and coworkers [74] designed an MOF-based EC aptasensor composed of MIL-101@AuNPs, hemin/G-quadruplex DNA enzyme (DNAzyme), and horseradish peroxidase (HRP) for the early detection of liver cancer, which improved the LOD of HepG2 cells up to 5 cells mL^{-1} with a wide range of 10^2 to 10^7 cells mL^{-1}. In addition to selective diagnosis, the designed aptasensor induced significant electrical signal amplification through synergistic cooperation of hemin/G-quadruplex DNAzyme and natural HRP. The G-quadruplex DNAzyme was prepared though the HCR method via connecting the thiolated TLS11a aptamer sequence (at the 3′ end) to two other sequences with 61 nucleotide bases. By the formation of hemin/G-quadruplex as a mimicking peroxidase the response of differential pulse voltammetry (DPV) improved significantly. Meanwhile, HRP by catalyzing hydroquinone in the presence of H_2O_2 effectively reduced the noise-to-signal ratio and accelerated electron transfer to improve the electrical signal [74]. In another study, it was determined that the

use of a duplex hairpin probe in S1-AuNPs@Cu-MOF-based EC aptasensors not only improved the LOD of miRNA-155 to 0.35 fM with a wide linear range from 1.0 fM-10 nM but also raised hopes to amplify the electrical signal significantly [75]. In this research, it was revealed that after opening the hairpin1 (H1) structure in the presence of miRNA-155 (target) and binding to the hairpin2 (H2) structure and completing the cyclic process by miRNA-155, a significant amount of H1–H2 is formed. Then, H1-H2 duplex aggregation improved the electrical signal based on the enhancement of electron transfer in the S1-AuNPs@Cu-MOF electrode [75]. Even though molecular biological technologies offer several significant advantages, including high efficiency, programmability, biocompatibility, non-toxicity, and non-immunogenicity, they still suffer from several problems such as low HCR sensitivity and time-consuming processes. Hence, a group of researchers focused on the catalytic activity of enzymes and even pseudo-enzymes due to their controllable function and high specificity. The functional mechanism of the enzymatic approach is focused on substrate degradation like a H_2O_2 and noise-to-signal ratio reduction, as well as faster electron transfer by enzymatic products. For example, Li and coworkers [76] by designing glucose oxidase (GOx)/HRP@ZIF-90 as a sensor containing ovarian cancer marker and creating a competitive reaction of ATP with Zn^{2+} to break the structure of MOFs to release GOx and HRP, were able to amplify the electrical signal through the enzymatic cascade reaction. The designed aptasensor increased the LOD of CA-125 up to 0.05 pg mL^{-1} with a wide range of 0.1 pg mL^{-1}–40 ng mL^{-1} along with high selectivity. In another study, it was reported that the combination of tyrosinase to calcined porous carbon-based ZIF-8 containing the PSA aptamer not only increased the LOD of prostate cancer to 0.01 ng mL^{-1} with a wide range of 0.01 to 50 ng mL^{-1} but also significantly improves the electrical signal based on the tyrosinase activity to catalyze the oxidation of electroinactive phenol to electro-active catechol and start the redox cycle under the influence of NADH [77]. Despite the timely and sensitive detection of biomarkers by the enzymatic approach in MOF-based sensors [78, 79], due to the complicated processes of enzyme immobilization on the electrodes and corresponding reduced enzyme, development of another strategy seems necessary. Electroactive nanohybrids with different physicochemical properties can be potentially used for the development of potential biosensing platforms via accelerating the electron transfer for signal amplification. The biocompatibility along with the fast response of nanohybrids in signal amplification has made the use of this approach interesting in the field. In this regard, Fu and coworkers [80] used AuPtRu trimetallic nanohybrids in Ce-MOF containing TSP-1 aptamer to boost the EC signal. In addition to H_2O_2 catalysis, the AuPtRu nanocomposite can function as a signal probe in this sensor. Therefore, the designed aptasensor has an improved LOD up to 0.13 fg mL^{-1} with a detection range of 1 fg mL^{-1} -10 ng mL^{-1} [80]. Furthermore, by using Au@self-polymerized dopamine (PDA)@Fe-MOF as a biocompatible EC aptasensor, Li and coworkers [81] were able to increase the LOD of CEA up to 0.33 fg mL^{-1} with a wide range of 1 fg mL^{-1} −1 μg mL^{-1}. The active sites in Fe-MOF and the combination of PDA-decorated AuNPs with this platform significantly accelerated the electron transfer on the electrode surface designed for signal amplification. Recently, an EC sensor resulting from the interaction of a covalent organic framework containing nitrogen-doped graphene nanocomposite (COF-NG) with a Fe-MOF decorated with AuNPs as a capture/signal probe was designed, which is capable of high electron transfer for non-small cell lung cancer detection with LOD of 7.65 fM and a linear range of 100 fM to 100 nM [82]. Guo and coworkers [82] illustrated that although COF-NG is favorable for electron transfer due to its porous structure and good conductivity, the integration of Fe-MOF with NG-COF increased the electrical signal by inducing the reaction of Fe^{3+} with $K_4[Fe(CN)_6]$.

Electrochemical (EC) sensing strategies

The biological analyte detection by EC biosensors is mostly based on potential [voltammetry: DPV, square wave voltammetry (SWV), cyclic voltammetry (CV), and linear sweep voltammetry (LSV)], current (amperometry), and conductivity (conductometry) assays. It seems that among the above strategies, voltammetry/potentiometry has received the most interest in the field. In addition to the above findings, the use of impedance (EIS: EC impedance spectroscopy) as well as the integration of EC methods with luminescence [electroluminescence (ECL), photoelectrochemistry (PEC)] also is of a great interest. These techniques have unique features such as signal measurement, mass transfer, and specific target selection (Table 1).

Aptamers and aptamers-modified MOFs

Aptamers

An aptamer is a single-stranded nucleic acid molecule with the ability to recognize specific targets and is classified based on origin, generating methods, and location of marker detection (on the tissue surface, biological secretions such as saliva, urine, and milk, and blood) [99]. Although various generating methods can be observed in the literatures [100], the use of the systematic evolution of ligands by exponential enrichment (SELEX) approach including 5 steps of binding, partitioning, washing,

Table 1 A summary of the mechanism, advantages and sensitivity of EC aptasensors in cancer detection

Class		Mechanism	Benefits	Sensitivity
Voltammetry	DPV	Applying amplitude potential pulses on a linear ramp potential where the selected base potential value has no Faraday reaction.	High signal-to- noise ratio, high sensitivity, low cost, portable, miniaturization capacity, using a wide range of samples, the possibility of checking solid and liquid samples, and remarkable repeatability.	Zr-MOF-on-Zn-MOF [target: protein tyrosine kinase-7 (PTK7)]: LOD of 0.66 pg mL^{-1} [60]; Cu-MOF-RGO (target: MUC1): LOD of 7.5 pg mL^{-1} [83]; MnO@C@AuNPs (target biomarker: MUC1): LOD of 0.31 pM [84].
	SWV	A large-amplitude differential method with wave form consisting of a symmetrical square wave that is superimposed on a base staircase potential applied to the working electrode.		HCR-Pb-MOF (target: CEA): LOD of 0.333 pg mL^{-1} [52]; BPNSs/Fc/ZIF-67/ITO (target: MCF-7 exosomes): LOD of ~100 particles mL^{-1} [85]; Au/Fe-MIL-88B-NH_2 (target: PSA): LOD of 0.13 pg mL^{-1} [86].
	CV	The working electrode potential is ramped linearly versus time and after the set potential, the working electrode's potential is ramped in the opposite direction to return to the initial potential.		AuNPs/Cu-MOF (target: HER2): LOD of 3.0 fg mL^{-1} [87]; NG-PEI-$COF_{TAPB\text{-}TFPB}$ (target: NSCLC): LOD of 7.65 fM [82]; MOF/PtNPs/G-quadruplex/hemin (target: MCF-7): LOD of 6 cells mL^{-1} [88].
Amperometry		Measuring the analyte based on the current or potential resulting from the chemical reaction of electroactive materials on the surface of the transducer.	Low cost, good sensitivity and selectivity, and high stability.	Fe_3O_4@TMU-21-MWCNT (target: HER2): LOD of 0.3 pg mL^{-1} [89].
Conductometry		The specific conductivity of an analyte is measured based on the monitoring of chemical reactions.	Fast, reliable, no reference electrode, cost-effective.	TCNQ-$Cu_3(BTC)_2$ (target: PSA): LOD of 0.06 ng mL^{-1} [90].
Impedance	EIS	Electron transfer capacity on the electrode by applying an electric field to induce the accumulation of ions around the analytes to change the surface polarization. Then, the analytes trapped on the electrodes change the electron transfer capacity.	Wide linear range, label-free, low cost, portability, real time detection, miniaturization, and readiness for lab-on-a-chip integration.	AgNC@Apt@UiO-66 (target: CEA): LOD of 8.88 pg mL^{-1} [91]; Cr-MOF@CoPc (target: CT26): LOD of 36 cells mL^{-1} [92]; Zr-MOFs (target: MCF-7): LOD of 31 cell mL^{-1} [93].
Luminescence	ECL	Response to electric current or electric field through an analyte and producing an optical phenomenon.	High range for target substrate, portability, easy storage, good reusability, low cost, rapid analysis, high sensitivity, high efficiency with MOFs, low background signal, wide dynamic response ranges, and chemical stability.	DNAzyme/gold nanorods (AuNRs)-complementary DNA (cDNA) (target: CEA): LOD of 0.036 pg mL^{-1} [94]; Hf-TCBPE/Fc-HP_3 (target: MUC1): LOD of 0.49 fg mL^{-1} [95]; Zn-PTC (target: microRNA-21): LOD of 29.5 aM [96].
	PEC	Converting the chemical energy caused by the analytes into electricity under light illumination.		Zn-MOF/AuNP/AgNS (target: CA153): LOD of 0.0275 U mL^{-1} [97]; Cu/UiO-66 (target: CEA): LOD of 0.01 ng mL^{-1} [98].

DPV differential pulse voltammetry, *SWV* square wave voltammetry, *CV* cyclic voltammetry, *EIS* EC impedance spectroscopy, *ECL* electroluminescence, *PEC* photoelectrochemistry, *LOD* limit of detection

amplification, and conditioning [101, 102] is of great interest. The use of cell-SELEX approach is highly recommended due to the binding of the generated aptamers even with unknown membrane receptors on the cell surface [103]. In this approach, the positive selection steps include incubation, washing, and amplification of binding aptamers, while the negative selection steps remove sequences that bind to normal cells. However, the production of reliable and stable aptamers along with the aptamer selection method is still under discussion. Because some challenges of this approach, such as the complexity of some cancer cell lines, changes in protein expression, and choosing the appropriate cell line have not been fully addressed. Therefore, the clinical successes of aptamers are not comparable to those of antibodies. While, aptamers are more stable than antibodies against pH, temperature, and ionic changes [104]. Despite the wide range of aptamers produced for cancer diagnosis (Table 2), aptamers have not been notably used in clinical trials for cancer diagnosis and are being mostly studied in the laboratory. For instance, in the field of assays, Landman's group (https://clinicaltrials.gov: NCT02957370) conducted a clinical trial for bladder cancer diagnosis based on aptamers and EC assays combined with calorimetry, the report of which is not available.

Functionalization of MOF with aptamers

Functionalized MOF NPs as structural analogue of MOF, could serve as excellent signal carriers for the development of aptasensors. Indeed, abundant functional moieties on the surface of MOF pores can result in selective absorption of a large number of metal ions [109–111]. Furthermore, modified terminated DNA can be easily adsorbed on functionalized MOF-NH_2 via the coupling and click reaction [112, 113]. For example, the first MOF developed NP-DNA biconjugate was mediated with a click reaction between dibenzylcyclooctyne-modified DNA and azide-modified MOF-N_3 [114]. The fabricated bioconjugates with 3D spherical architecture displayed low cytotoxicity and improved stability. As a result, the stability of the signal transporters can be achieved through development of DNA-metal ions-MOF bioconjugates.

Also, Guo et al. aimed to fabricate Apt-templated AgNPs bioconjugated with Zr-MOF aptasensors through establishment of Zr−O−P interaction between MOF and the DNA strands for bifunctional EC and SPR-based detection of CEA biomarker [91]. In addition to improved biocompatibility and potential EC properties, the fabricated nanoplatform demonstrated favorable bioaffinity and excellent reproducibility. It was also shown that the developed nanoconjugates had a LOD of 8.88 and 4.93 $pg{\cdot}mL^{-1}$ derived EIS and DPV, respectively, over a wide linear range of the CEA concentration (0.01–10 $ng{\cdot}mL^{-1}$).

In general it can be suggested that functionalization of MOF with aptamers can be done through formation of Au-S bond [115], streptavidin-biotin binding [116], coordination between PO_4^{3-} moiety and MOF [117], π-π interaction and hydrogen bonding [118], covalent binding mediated with click chemistry [119], and covalent interaction through EDC/NHS linking [120]. For further

Table 2 A sample of aptamers used in the diagnosis of different types of cancers [105–108]

Nr.	Aptamers	Target	Cancers
1	S2.1	MUC1	Breast, lung, ovarian, pancreatic cancers, etc.
2	AFP-apt	Alpha fetoprotein	hepatocellular carcinoma
3	HB5, A30	HER2/HER3	Breast, gastric, lung, colorectal, esophageal, ovarian cancers, prostate, pancreatic, etc.
4	ESTA	E-selectin	Breast, some of metastasis
5	E0727, TuTu2231, KD1130, CL428	EGFR	Squamous cell carcinoma, breast, glioblastoma multiforme, lung, etc.
6	NOX-A12, NOX-E-36	CXCL12	Multiple myeloma, leukemia, glioblastoma multiforme
7	SYL3, EpDT3-DY647	EpCAM	Bladder, breast, colon, lung, ovarian, pancreas, prostate, etc.
8	NX-191, NX-213, Vap7, V7t1	VEGF	Lung, breast, brain, colon, pancreatic, melanoma, myeloid, gastric, etc.
9	PSMA-4-1BB	CD137	Prostate
10	xPSM-A10, A9g	PSMA	Prostate, bladder, kidney, etc.
11	ARGO100	NF-kB	Prostate, cervical, lung, breast, etc.
12	AS1411, FCL-II	Nucleolin	Leukemia, lung, renal, breast, pancreatic, etc.
13	PNDA-3	Periostin	Breast
14	ARC126, AX102	PDGF-B	Vessel, endothelial cells, retinal
15	CD40apt	CD40	Bone marrow

information the readers are referred to a comprehensive review reported by Liu, and coworkers [121], which described functionalization of MOF with DNA and amino acids for different applications.

Core-shell MOF-based aptasensors

By conjugating EC aptasensors with different metallic signal tags, it has been possible to detect different biological or chemical reactions with high sensitivity [122, 123]. The development of metals-tagged aptamers is classified into two main categories: the application of pure metal NPs [124, 125], and the development of a core-shell platform with integration of metal ions into MOF NPs with a highly specific surface area [126]. Relative to the former strategy, the latter one could be utilized to develop more different types of metals-tagged aptamers owing to the modification of MOFs with multiple electroactive metal ions, including Pb^{2+}, Cd^{2+}, Cu^{2+}, and Zn^{2+} [49].

Indeed, in order to develop aptasensors, it's crucial to utilize appropriate substrates to tag aptamers and load sufficient metals for signal intensification. Because of its excellent adsorption properties and diverse amine and carboxyl grafting moieties, the porous MOF may be an ideal candidate for promoting the co-adsorption of substances [127, 128]. Particularly suitable candidates for the development of aptasensors are MOF NPs with good colloidal stability and a large reactive surface area. Several MOF -based aptasensors have also been developed for optical cancer biomarker detection [129–131]. Nevertheless, the application of MOF NPs to develop potential core-shell sensitive EC aptasensors for the detection of cancer biomarkers is still considered as a new area of research.

Furthermore, metal ion leakage is a significant disadvantage of metal ion adsorption on MOF as signal tags. Indeed, the interaction between metal ions and MOFs is almost entirely mediated by weak non-covalent forces, resulting in significant metal ion leaching and the inevitable generation of background (false positive) signals, reducing the specificity of this approach. Although several sensitive EC aptasensors using metallic nanotags with MOFs as carriers were developed for the detection of cancer biomarkers in recent years, it is difficult to remove the metal ion leakage mediated by MOF NPs-supported metallic signal tags. Metal ion incorporation into the MOF could be one possible approach, which is expected to result in a stable core-shell structure and low metal leakage. Indeed, when compared to traditional catalysts, MOF-based derivatives reduce metal leakage due to the protection of carbon atoms in the core-shell structure [132, 133]. Furthermore, the deposition of MOF-based nanostructures with polymers and various porous materials could be an effective method for addressing metal leakage [134].

Application of core-shell MOFs in the detection of tumor antigens

Prostate-specific antigen (PSA)

The tactics by utilizing synergetic core-shell MOF nanostructures as signal probes furnish a potential platform for expanding uncomplicated, rapid, and ultrasensitive dual-channel uniform aptasensors, which display an excellent prospective as promising platforms in cancer diagnosis.

Bhardwa et al. developed tetracyanoquinodimethane (TCNQ)- doped Cu-MOF, $Cu_3(BTC)_2$, adsorbed on Au electrodes, an immune-EC biosensing system, for exceptionally sensitive sensing of a PSA with a LOD of 0.06 ng mL^{-1} and wide linearity of antigen between 0.01 and 150 ng mL^{-1} [90]. Based on the published reports for PSA detection by other platforms, including SiO_2 NPs (LOD = 0.76 ng mL^{-1}) [135], microwell SWCNT (LOD = 0.001 ng mL^{-1}) [136], graphene-modified GC (LOD = 0.008 ng mL^{-1}) [137], graphene/methylene blue nanocomposite (LOD = 0.013 ng mL^{-1}) [138], MoS_2 (LOD = 0.001 ng mL^{-1}) [139], graphene/Au (LOD = 0.59 ng mL^{-1}) [140], GOQDs (LOD = 0.0003 ng mL^{-1}) [141], MXene-Au-MB (LOD = 0.00008 ng mL^{-1}) [142], DNA tetrahedron structural probes (TSPs)-Au nanoflowers (NFs)-modified screen-printed electrodes (SPEs) (LOD = 0.2 ng mL^{-1}) [143], the LOD of this MOF-based biosensor is comparable with others. However, other platforms, such as carbon QDs-AuNPs with a LOD of 2 fg mL^{-1} [144] and hierarchical SiO_2@MoS_2 nanostructures with a LOD of 2.5 fg mL^{-1} [25], have recently

Table 3 Core-shell MOF-based EC apta/sensor for ultrasensitive PSA detection

Platform	LOD	Linear range	Detection type	Refs.
AgNC@Apt@UiO-66	8.88 and 4.93 pg·mL^{-1}	0.01–10 ng·mL^{-1}	EIS and DPV	[91]
Au-hemin-Mil-DNAzyme	0.058 ng mL^{-1}	0.5 to 500 ng mL^{-1}	EIS	[147]
PdNPs@Co-MOF	0.03 pg mL^{-1}	0.01 fg.mL^{-1} to 50 ng. mL^{-1}	EIS	[148]
Pd@hollow Zn/Co core–shell ZIF67/ZIF8	0.78 pg mL^{-1}	5 pg mL^{-1} to 50 ng mL^{-1}	EIS	[149]

demonstrated significantly lower LOD than that of TCNQ- doped Cu-MOF. Therefore, optimization of fabricated core-shell platforms may be a potential strategy for biomarker detection [145, 146].

Table 3 also summarizes the application of core-shell MOF NPs in the design of apta/biosensor for ultrasensitive PSA detection.

Carbohydrate antigen 15 − 3 (CA15-3)

CA15-3 could represent a potential tumor marker in several types of cancers such as ovarian, lung, and prostate, as well as benign breast cancer. Xiong and and coworkers [150] developed an ECL immunoassay for CA 15−3 detection by using $Ru(bpy)_6^{2+}$-functionalized amino-coated UiO-66 MOF NPs. Ru derivatives were used as a luminescent probe, with UiO-66-NH2 acting as a carrier and Nafion as a fixer (Fig. 1a). Also, the covalent conjugation of CA 15 − 3 Ab was mediated by amide reaction. It was discovered that the ECL signal was apparently quenched after the CA15-3 marker interacted with the immunosensor, and the LOD was in the range of 5×10^{-4} to 5×10^{2} U mL^{-1} and a LOD of 1.77×10^{-5} U mL^{-1}, which was applicable in real samples [150]. Also, a signal amplification procedure mediated by initiated radical polymerization activated with coupling cascade catalysis was introduced for ultrasensitive sensing of CA15-3 through EIS immune-based assay [151]. As immune-based probes, Cu-MOF as a peroxidase-mimic enzyme in combination with Ab and GOx, generation of H_2O_2, was able to initiate radical polymerization via cascade catalysis. Indeed, resistance values improved following the interaction of H_2O_2 with acetylacetone catalyzed by Cu-MOF and the formation of acetylacetone radicals-based poly N-isopropylacrylamide (Fig. 1b). This biosensor detected CA15-3 at detection ranges ranging from 10 μU mL^{-1} to 100 mU mL^{-1} with a low LOD of 5.06 μU mL^{-1} for CA15-3 [151]. It should be noted, however, that both platforms serve as immunobiosensors that rely on Abs, which present some challenges in biosensor development, such as partial denaturation and orientation. As a result, the drawbacks of Ab-based biosensors can be addressed by using another strategy, aptasensors, which needs further investigations in the future studies.

Carcinoembryonic antigen (CEA)

A high level of CEA could indicate several types of cancer, including colorectal, prostate, ovarian, lung, thyroid, and liver cancer. Zhou and coworkers [152] described a GOx-mediated cascade catalysis for the development of an ultrasensitive EIS aptasensor catalyzed by Pt@MOF NPs and hemin/G-quadruplex (hGq) as peroxidase-mimic enzyme for the oxidation of conductive 3,3-diaminobenzidine (DAB) and the generation of insoluble precipitates with minimum conductive properties, with a low LOD of 0.023 pg mL^{-1} toward CEA (Fig. 2a) [152]. Guo and coworkers [91] also reported an AgNP@Apt@Zr-MOF platform for the development of bifunctional EC and optical aptasensors toward CEA with LODs of 4.93–8.88 pg·mL^{-1} and 0.3 pg·mL^{-1}, respectively and a broad linear range of the CEA concentration (0.01–250 ng·mL^{-1}) [91]. Therefore, the synthesis route of MOF, structure, and type of MOF can play a key role in the sensitivity of MOF-based biosensors in detection of biomarkers. Also, by using MOFs as a nanocarrier of EIS active materials (methylene blue) along with controllably assembled DNA, gatekeeper, a smart platform based on target (CEA)-guided cascade boosted release of methylene blue was developed which was able to detect CEA with a LOD of 16 fg mL^{-1} and broad linear range of 50 fg mL^{-1} to 10 ng. mL^{-1} [153]. Furthermore, Li and coworkers [81] developed an EC aptasensor composed of self-polymerized dopamine modified Au coordinated with Fe-MOF (abbreviated as: Au@PDA@Fe-MOF) for the detection of CEA with improved sensitivity, several active sites, good biocompatibility, and potential selectivity derived from several −COOH groups and Fe^{3+} sites in porous and on the surface of Fe-MOF, respectively. Then, NH_2-modified CEA-selective aptamer and redox PDA along with Fe-MOF could accelerate the electron transfer for dual signal intensifying [81]. The developed aptasensor had a broad antigen detection range from 1 fg mL^{-1} to 1 μg mL^{-1} with a LOD of 0.33 fg mL^{-1}. Moreover, a label-free ECL aptasensor for ultrasensitive detection of CEA was developed based on CdS QDs-modified MOF and triethanolamine-modified AuNPs as bi-coreactants of $Ru(bpy)_3^{2+}$ ECL platform, as well as a carrier for aptamer (Au–S bond) (Fig. 2b) [154].

Human epidermal growth factor receptor-2 (HER2)

Approximately 20–30% of breast tumors upregulate the expression of HER2. The bimetallic ZrHf-MOF embedded with carbon dots (abbreviated as CDs@ZrHf-MOF) was used as a potential systems for the detection of HER2 in MCF-7 cancer cells through EC aptasensor with a LOD of 19 fg mL^{-1} (Fig. 3a) [155]. It was seen that LOD of other biosensors for HER2 detection including Au nanostructured screen-printed graphite [156], CuO NPs [157], AuNP-based rolling circle amplification [158], ferrocene-labeled DNA/Au [159], polycytosine DNA [160], aptamer-based interdigitated electrode [161], antiHER2/APTMS-Fe_3O_4 [162] were 6.0 pg mL^{-1}, 0.956 pg mL^{-1}, 80 fg mL^{-1}, 4.9 ng mL^{-1}, 0.5 pg mL^{-1}, 0.1 ng mL^{-1}, 0.02 pg mL^{-1}, respectively.

Also, a magnetic Fe_3O_4@ TMU-21-MWCNT with redox activity toward H_2O_2 was used as a potential

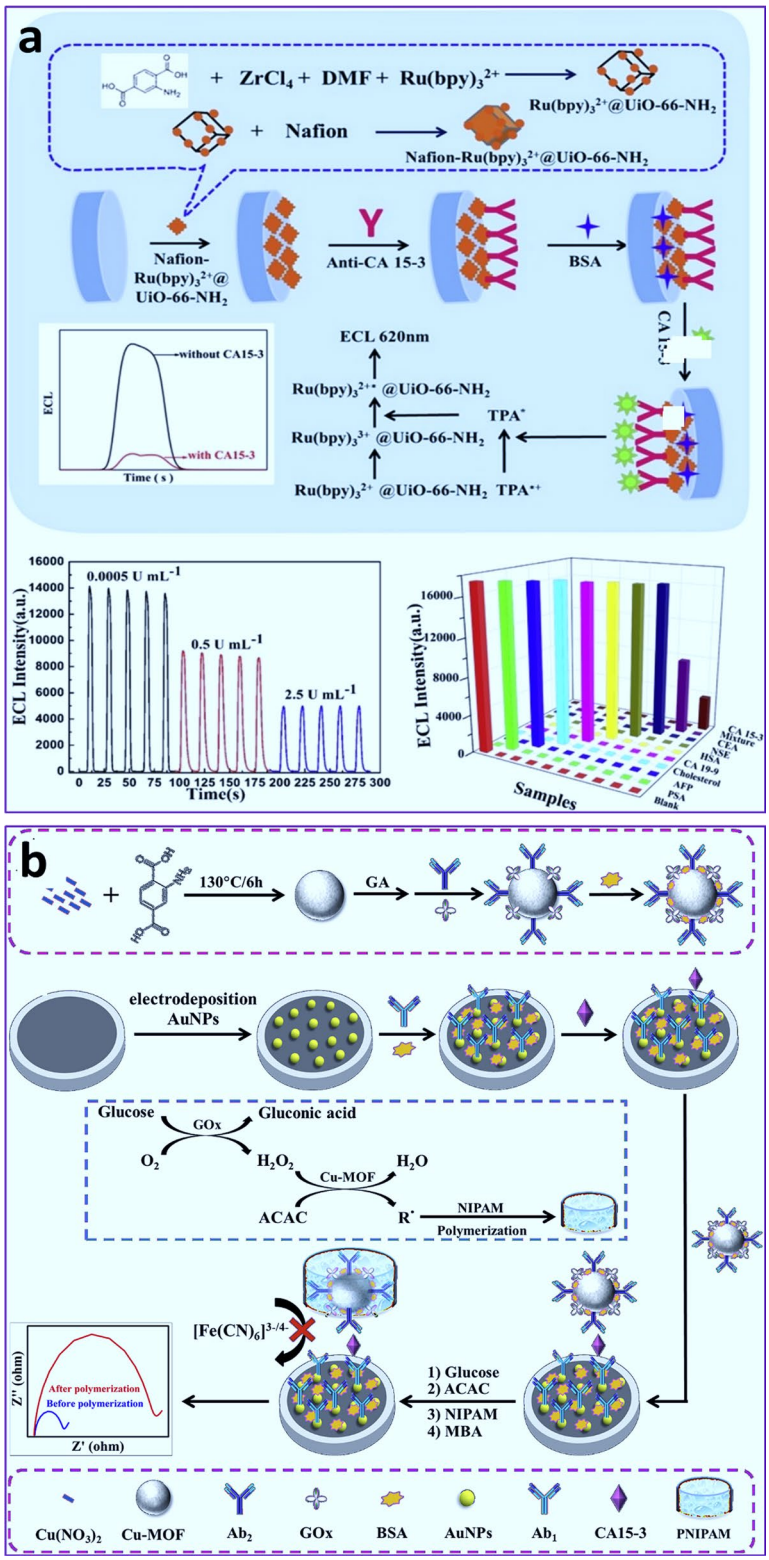

Fig. 1 **a** Schematic illustration of an ELC immunoassay for CA 15−3 detection by using $Ru(bpy)_6^{2+}$-functionalized amino-coated UiO-66 MOF NPs [150]. Reprinted with permission from Ref. [150], copyright 2019, Elsevier. **b** Schematic illustration of immune-based MOF EIS biosensors for cascade catalysis-initiated radical polymerization-stimulated signal intensification for CA15-3 detection [151]. Reprinted with permission from Ref. [151], copyright 2019, Elsevier. *GOx* Glucose oxidase, ***ACAC*** acetylacetone, *PNIPAM* poly (N-isopropylacrylamide)

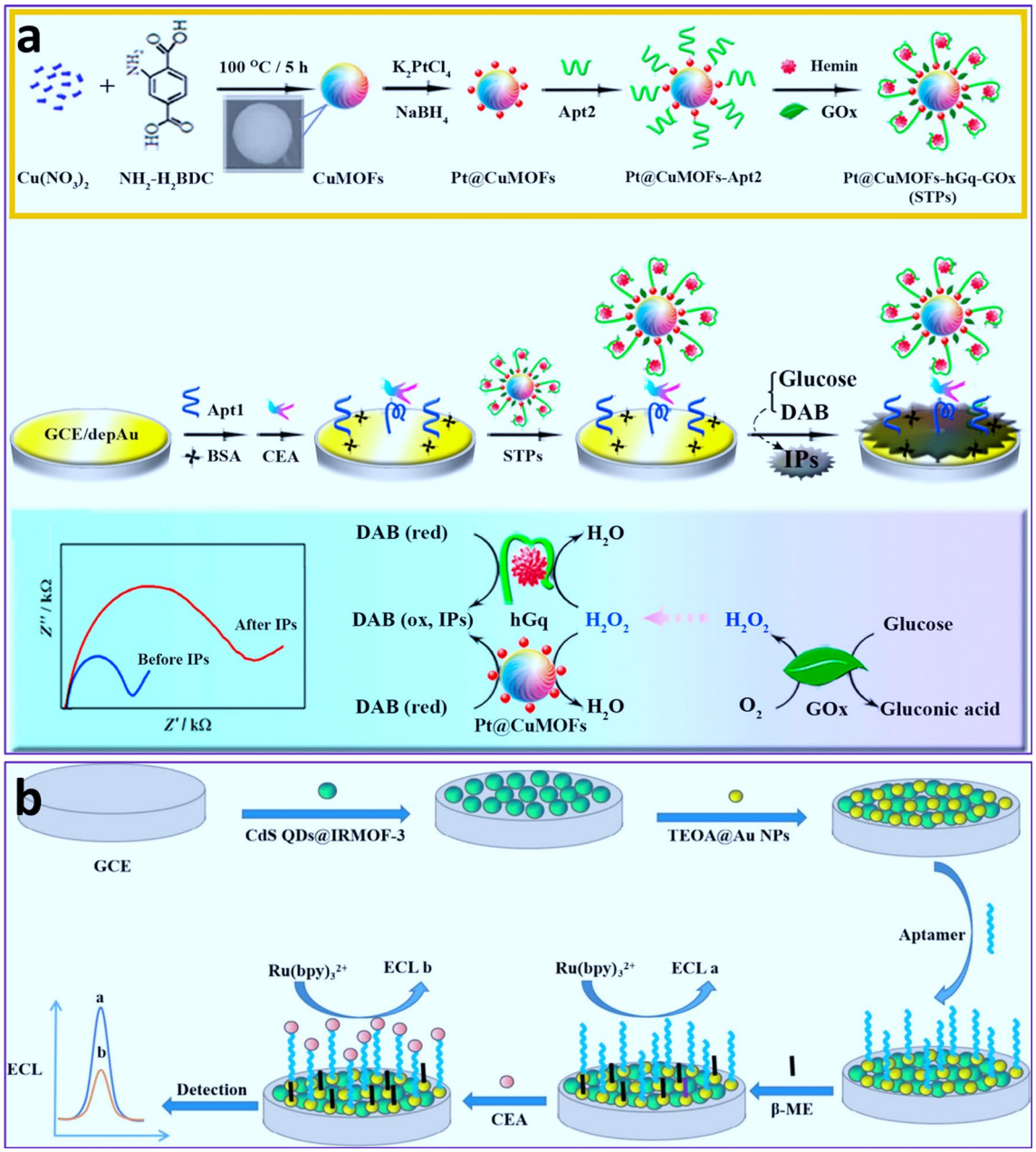

Fig. 2 **a** Schematic illustration of core-shell MOF-based EIS aptasensor for cascade catalysis-initiated radical polymerization stimulated signal intensification for CEA detection [152]. Reprinted with permission from Ref [152], copyright 2017, Elsevier. **b** Schematic illustration for the fabrication of CdS QDs@MOF and TEOA@Au aptasensor for CEA detection [154]. Reprinted with permission from Ref. [154], copyright 2022, Elsevier. *IPs* Insoluble precipitates, *DAB* 3,3-diaminobenzidine, *TEOA* triethanolamine

immunosensor against HER2 [89]. Indeed, with HER2 biomarker the amperometric current of H_2O_2 changes, which could be a sign of antigen–Ab interaction on the electrode with a linear range of 1.0 pg mL^{-1}-100 ng mL^{-1} and LOD of 0.3 pg mL^{-1} (Fig. 3b) [89]. Although the detection of HER2 is well-correlated with human serum samples, the use of immune-based biosensors due to some challenges such as low stability and sensitivity may limit their clinical application. For example, it has been reported that aptasensors outperform immunosensors in terms of sensitivity, reusability, and storability against HER2 detection [163].

It was shown that the LOD of Fe_3O_4@TMU-21-MWCNT for the detection of HER2 via amperometric method was significantly lower than those of Hyd–AuNP – Apt (SWSV, 37 pg mL^{-1}) [124], Au

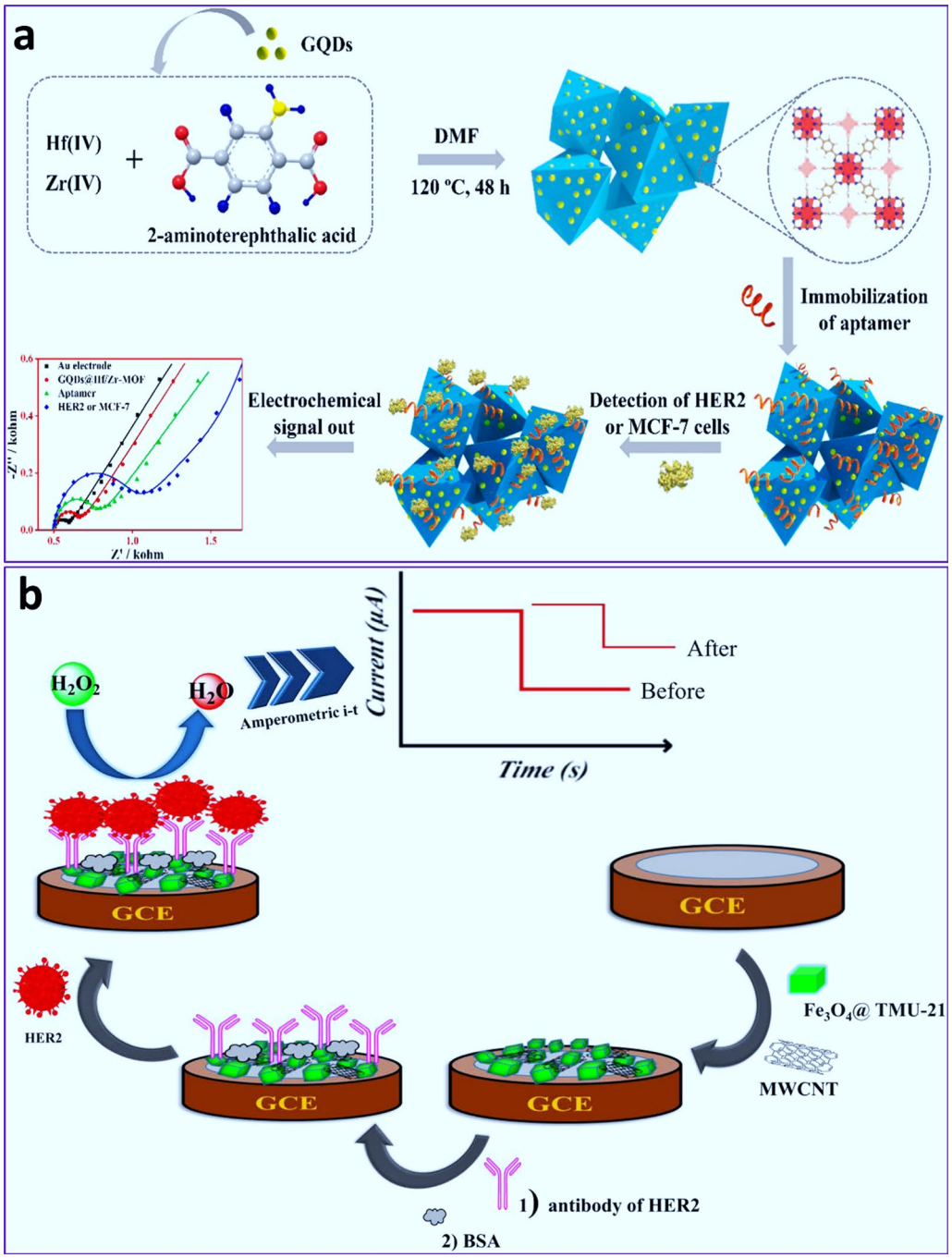

Fig. 3 **a** Schematic illustration of the synthesis of CDs@ZrHf-MOF-based aptasensor for the detection of HER2 [155]. Reprinted with permission from Ref. [155], copyright 2019, Elsevier. **b** Schematic illustration of the synthesis of Fe_3O_4@TMU-21-MWCNT-based immunosensor for the detection of HER2 [89]. Reprinted with permission from Ref. [89], copyright 2020, Elsevier. *CDs* Carbon dots, *BSA* bovine serum albumin

NPs-modified disposable screen-printed carbon electrodes (impedimetric, 0.01 ng mL^{-1}) [164], inkjet printed Au working 8-electrode array (amperometry, 12 pg mL^{-1}) [165], streptavidin-alkaline phosphatase (LSV, 0.16 ng ml^{-1}) [166], Ab2-PbS QDs (SWV, 0.28 ng mL^{-1}) [167], and CdSe@ZnS (DPV, 2.10 ng ml^{-1}) [168]. However, some other biosensor platforms have been reported to outperform Fe_3O_4@ TMU-21-MWCNT sensor for the detection of HER2 such as anti-HER2 conjucated mesoporous ZnO nanofibers

(EIS, 185 fg ml^{-1}) [169], hierarchical composite of porous graphene and TiO_2 nanofibers (EIS, DPV, 185 fg ml^{-1}) [170], and Fe_3O_4–Au NPs–AgNPs (DPV, 20 fg ml^{-1}) [162].

Cancer antigen 125 (CA-125)

The CA-125 detection can be applied to detect early signs of ovarian cancer. Serval biosensors such as FA-HCl-doped polyaniline-chitosan-Ag-Co3O4 nanosheets [171], MoS_2-Au-nanoflowers [172], Au NP-ZnO nanorods [173], graphene polyaniline [174], 3D Au electrode [175], benzothiophene derivative [176] have been developed for sensitive EC determination of CA-125 with an LOD ranging from 0.25 pg mL^{-1} to 2.5 ng mL^{-1}. Regarding the apparent biosensing properties, advanced EC performance, and exceptional biocompatibility of Fe-/Tb-MOF, as well as fluorescence properties of Tb-MOF, the hetero-architectured core-shell bimetallic TbFe-MOF could be developed and recruited as an advance system to immobilize aptamer strands for concurrently sensing cancer biomarkers and living cancer cells (Fig. 4a) with a LOD of 0.000058 U·mL^{-1} via EIS detection method [177]. The developed biosensor showed a potential binding of aptamer with CA-125 biomarker evidenced by an apparent decrease in current (preventing electron transfer at electrode-solution interface) and an increase in ΔEp [177].

It was found that other biosensors including microfluidic origami device [178], mercaptopropionic acid/AuNP@SiO_2/CdSe QD [179], multi-functionalized g-C_3N_4 [180], Au nanostructures [181], phosphoserine imprinted CNT nanosensor [182], chitosan-AuNPs/multiwall carbon nanotube/GO [183] with different detection methods show a LOD in the range of 0.0016 to 5.5 U·mL^{-1}, which is not comparable with that of TbFe-MOF [177].

In another study, tricopper benzene-1,3,5-tricarboxylate (CuBTC) CuBTC@MoS_2-AuNPs/CA125 Ab-functionalized electrodes were developed, where MoS_2 and AuNPs were used for enhancing the electron transfer capability and attachment of Ab, respectively. Therefore, based on the significant synergistic effect-derived EC signal, the modified CuBTC@MoS_2-AuNPs/CA125 Ab electrode was able to detect CA125 with a LOD of 0.0005 U mL^{-1} and a broad linear range of 0.5 mU mL^{-1} to 500 U mL^{-1} by DPV [184]. It was shown that other EC immunosensors including mercaptopropionic acid/AuNP@SiO_2/QD [179] and chitosan-AuNP/MWCNT/ GO [183] show LODs (U mL^{-1}) of 0.0016 and 0.002, respectively for CA-125, which were

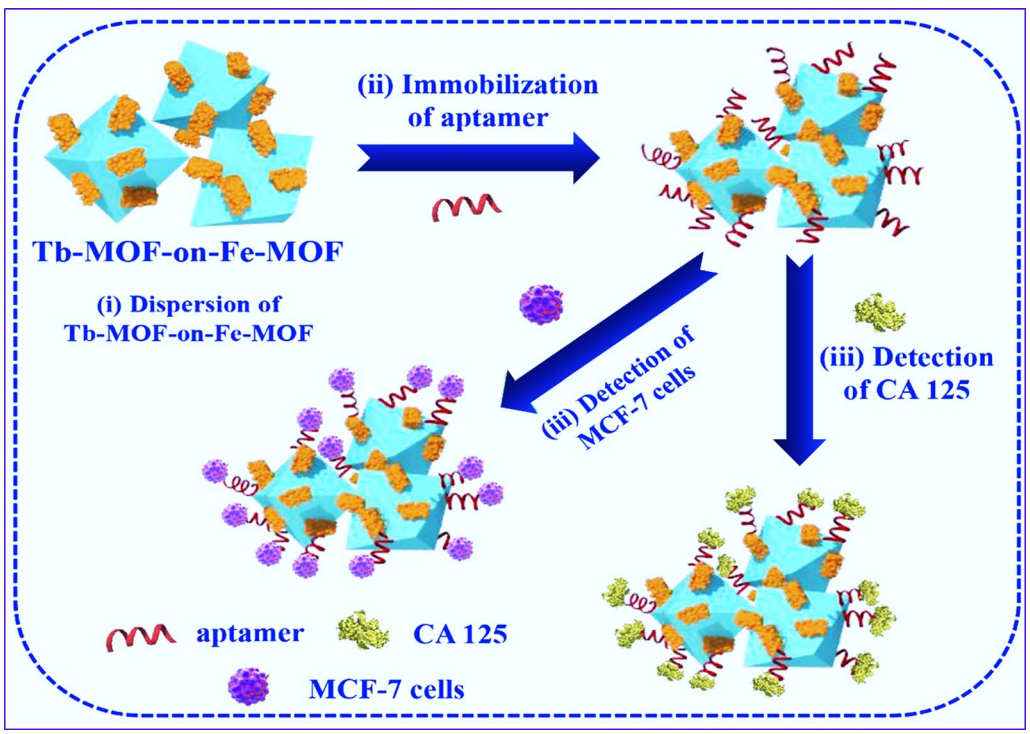

Fig. 4 Schematic illustration of core-shell bimetallic TbFe-MOF for the immobilization of the aptamer strands for concurrently sensing CA-125 and living cancer cells [177]. Reprinted with permission from Ref. [177], copyright 2019, Elsevier

significantly higher than that of CuBTC@MoS_2-AuNPs/CA125 Ab [184]. However, it has been reported that Fe_3O_4@g-C_3N_4-based EC immunosensor with a LOD of 0.0004 U mL^{-1} [180] shows comparable outcomes with CuBTC@MoS_2-AuNPs/CA125 Ab [184].

Cytokeratin 19 fragment (CYFRA21-1)

The CYFRA21-1 is known as an important tumor marker, particularly for lung cancer. Different EC-based platforms such as BSA/Anti-Cyfra-21-1/ncCeO$_2$-RGO/ITO [185], GCE/Fe_2N/rGO/Au-HWR/Ab1/BSA/CYFRA21-1/Ab_2-apoFt@Ir $(ppy)_3$ [186], Au-pThi/anti-CYFRA21-1/CYFRA21-1/anti-CYFRA21-1/Au/3D-G/GCE [187], and GCE/nafion-AuNPs/Ab_1/BSA/CYFRA21-1/Ab_2-TB-AuNPs@MoS_2@$Ti_3C_2T_x$ [188] with LODs (pg mL^{-1}) of 0.625, 0.43, 180, and 0.03 have been reported for the detection of CYFRA21-1 marker. Literature survey showed that, although there is no report on the simultaneous use of aptamers and MOF for EC-based detection of CYFRA21-1, there were several reports on the EC immunoassay. For example, Xu and coworkers [189] aimed to develop a feasible and ultrasensitive immunosensor based on complexation competition reaction between $CaCO_3$ NP-Au modified with Ab, ZIF-8, and EDTA for EC detection of CYFRA21-1. Excessive EDTA was used in the complexation reaction with $CaCO_3$ NPs and for etching ZIF-8 and AgNPs (signal amplifier) and ZIF-8 (signal silencer) onto the electrode surface. Because of the EDTA-based destruction of ZIF-8, the LSV signal of AgNPs was amplified (Fig. 5a) [189]. As a result, the amount of CYFRA21-1 modified with magnetic beads was quantified by analyzing the current signal of AgNPs, with a LOD of 3.175 fg mL^{-1} and a broad detection range of 10 fg mL^{-1} to 1 μg mL^{-1}. Also, a $Ru(bpy)_3^{2+}$ encapsulated cyclodextrin-based MOF with good biocompatibility was developed for ultrasensitive ECL detection of CYFRA21-1 in serum and A549 lung cancer cells, with a LOD of 0.006 ng mL^{-1} and a broad liner range of 0.1–50, 50–200 (ng mL^{-1}) (Fig. 5b) [190]. Furthermore, the sandwich-typed Tb-Cu-m-phthalic acid (PA) lanthanide MOF immunoplatform was used as a potential ECL-based platform for the detection of CYFRA21-1, where captured Ab was immobilized on Pd NPs functionalized Ni-Co layered double hydroxide (Pd-ZIF-67@LDH) nanostructures with high electrocatalytic activity for intensifying the ECL signal (Fig. 5c) [191]. The developed platform showed a broad linear range of 0.01–100 ng mL^{-1} and a low LOD of 2.6 pg mL^{-1} [191]. Comparison between ECL immunosensor and other strategies for CYFRA 21 − 1 detection indicated that ECL detection method provide a lower LOD (0.0026 ng mL^{-1}) in comparison with other EC detection methods with LOD in the range of 0.043–0.122 ng mL^{-1} [192–194].

Other tumor markers

Zhou and coworkers [60] reported the synthesis of two types of bimetallic ZnZr-based MOFs through MOF-on-MOF strategy and used them as a platform for immobilization of aptamer to develop a sensitive aptasensor to detect the cell membrane PTK7 as a tumor marker. It was seen that the developed core-shell hybrid bimetallic MOF was able to detect PTK7 marker with a LOD of 0.84 pg mL^{-1} and 0.66 pg mL^{-1} with detection range of 0.001 − 1 ng mL^{-1} through EIS and DPV, respectively.

Therefore, it was assumed the Zn-MOF-on-Zr-MOF could serve as a potential platform to provide higher signal output relative to the Zr-MOF-on-Zn-MOF platform [60]. Then, it was seen that Zn-MOF-on-Zr-MOF architecture decorated with aptamer can show higher sensitivity for the detection of PTK7 relative to structure-switching aptamer [195], [Ir(pbi)2(5,5-dmbpy)]PF6 [196], DNA-AuNPs/aptamer/AuNPs/Nf [197], DNA-AgNCs [198] with fluorescence, luminescence, DPV, and fluorescence detection methods, respectively. Indeed, it was discovered that the LOD of the above-mentioned method was in the range of 0.048-13 ng mL^{-1}, whereas the LOD of Zn-MOF-on-Zr- MOF was in the range of 0.66–0.84 pg mL^{-1}. Also, early detection of platelet-derived growth factor-BB (PDGF-BB), an important protein marker upregulated in tumor cells, can provide useful information for treatment of a broad range of cancers. Based on this theory, Li and coworkers [199] developed a potential core–shell nanostructure containing Cu-based MOF (Cu-MOFs) as well as COFs (TpBD) to be used as a potential platform for fabrication of an aptasensor for the detection of PDGF-BB. The Cu-MOFs (core) and TpBD (shell) were used in signal amplification and immobilization of PDGF-BB biomarker with a LOD of 0.034 pg mL^{-1} within the detection ranges of 0.0001 to 60 ng mL^{-1} [199]. Therefore, it was claimed that concurrent application of MOFs and COFs, as well as the adsorption of tumor marker-specific aptamer via different

(See figure on next page.)

Fig. 5 **a** Schematic illustration of the complexation competition approach for the detection of CYFRA21-1 based on ZIF-8 [189]. Reprinted with permission from [189], copyright 2020, Elsevier. **b** Schematic illustration of the synthesis of the CD-MOF@$Ru(bpy)_3^{2+}$ nanostructure for detecting CYFRA21-1 using an ECL strategy [190]. Reprinted with permission from Ref. [190], copyright 2021, Elsevier. **c** Schematic illustration of immunosensor and ECL detection of CYFRA21-1 [191]. Reprinted with permission from Ref. [191], copyright 2022, Elsevier. *CD* Cyclodextrin, *Pd-ZIF-67@LDH* Pd NPs functionalized Ni-co layered double hydroxide, *MBs* magnetic beads

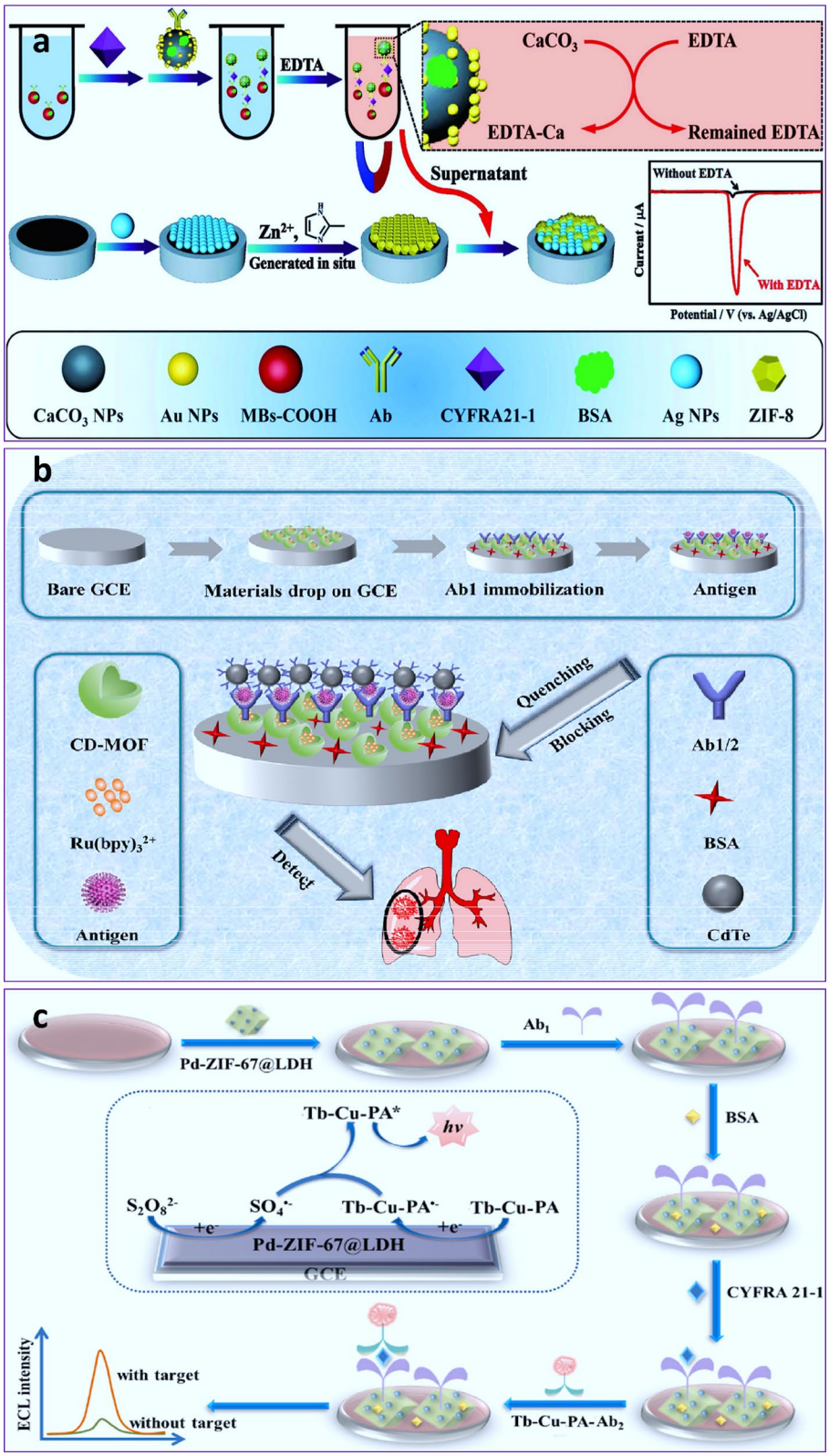

Fig. 5 (See legend on previous page.)

hydrophobic and hydrophilic interactions, could result in the fabrication of a potential core-shell-based aptasensor that can be used as a productive strategy to fabricate a biosensor for the feasible, accurate, and selective determination of a specific biomarker in clinical settings.

Conclusions and future perspectives

Promising results of EC aptasensors based on core-shell MOFs have enabled us to detect cancer biomarkers in a more accurate and sensitive manner in comparison with standard approaches. This category of aptasensors with the high loading of probes due to the increase of the surface-to-volume ratio and interconnected cavities along with the resistance of probes against destruction, were able to improve the selectivity, sensitivity, LOD, mass transfer and signals amplification of MOFs-based EC aptasensors compared to other electrodes. There are, however, some challenges needed to be addressed to make core-shell MOD-based EC aptasensors effective in clinical settings, including:

A positive or false negative signals: Because MOFs have a porous structure with high accessible surface areas, non-specific adsorption of biomaterials can negatively influence the assay. Thus, being able to manipulate the pore structure of MOFs during growth is a crucial requirement. Increasing the binding sites of target analytes by modifying the functional groups on surfaces seems like an effective way to reduce the binding of other biomaterials.

Biocompatibility: The catalytic activity outcomes reveal a significant increase in the catalytic performances of monometallic MOFs after incorporation of another metal or carbon atom in the same platform as well as an excellent enhancement in EC properties. However, commercializing this type of aptasensor is challenging because of biocompatibility and biodegradability issues.

Controllable dimensions and shapes: As expressed in many reports, the effects of morphology and size of MOFs on their functions have not been studied analytically, which can limit their practical application. Since nanoscale dimensions with polyhedral morphology can affect the performance of sensors [200, 201], it appears that producing a core-shell MOF-based EC aptasensor with uniform distribution improves sensitivity and accuracy mediated by boosting electron transfer.

Complex and expensive production: One of the most important challenges in the development of core-shell MOF-based EC aptasensors is the costly, complicated production on large scale, as well as insufficient accuracy and efficiency of these platforms in clinical applications due to the use of various ligands and aptamers in one platform compared to standard biosensors. Because detecting cancer with a single aptamer is fraught with false positive test results, the use of multifunctional core-shell MOFs-based EC aptasensors with multiple aptamers to simultaneously detect two or three targets is currently considered a potential strategy to address this issue.

Reproducibility and stability: Due to a lack of complete understanding of MOF growth mechanisms on electrode surface, designing electrodes with the controllable pores and structures that provide stability, electron transfer, and uniform electrocatalytic performances for clinical diagnostics is not possible. The integration of multiple NPs in MOFs, which can improve electron conductivity and catalytic activities, may provide some merits to overcome this concern. However, due to the lack of complete understanding of the synergistic effect of NPs with MOF and their effect on the loading of aptamers along with the excessive stability of NPs in the environment, it faces further challenges when it comes to their use in clinical settings.

Large-scale production: Potential immobilization and conjugation of aptamers on core-shell MOFs is a critical concern that should be properly addressed for the clinical diagnostics of biomarkers. The lack of comprehensive studies on the stability of core-shell MOF-based EC aptasensors, as well as their effect on diagnostic accuracy, has rendered the large-scale production of analogous sensors impossible. In fact, it is complicated to engineer the conformation, configuration, density, and stability of aptamers upon conjugation with core-shell MOF NPs. While, the interaction of aptamers on the surfaces and probably their spatial structure changes are a function of the inherent behavior of the nucleic acid sequences and their different interactions with the surface properties of the platform. It's undeniable that these effects can greatly reduce, if not stop, the accuracy and sensitivity of diagnosis in the clinical applications. A theory-based approach combined with computational methods can provide a more accurate assessment of the aptamer 3D configuration on the core-shell MOF NPs in the initial phase.

Overall, it appears that core-shell MOF-based EC aptasensors will become increasingly practical in clinical applications as a result of the efforts made to address the challenges.

Acknowledgements

We appreciate all colleagues contributed in discussion of this review paper. Moreover, our special thanks to the JNB, editors and reviewers for constrictive comments that has definitely increased the scientific integrity of this paper.

Author contributions

SK, AH, MMNB contributed in conceptualization, literature survey, and preparing the draft. WCC, AS and SHH contributed in literature survey, edition,

proofreading, and preparing the draft. MF, LAJA, TLMH and XL contributed in conceptualization, literature survey, preparing the draft, and supervision. All the authors reviewed the manuscript. All authors read and approved the final manuscript.

Funding
This project was partly funded by Kuwait University grant number, SC 14/18. Also, we acknowledge Henan Province International Science and Technology Cooperation Project, (NO: 232102520025) (S.K), 2021 Young and Middle-Aged Academic Leaders of Health in Henan Province, (NO: HNSWJW-2021001), and Program for Science & Technology Innovation Talents in Universities of Henan Province, (NO: 22HASTIT047).

Availability of data and materials
No data was used for the research described in this review article. This paper presents figures that do not belong to the authors; they have been reprinted with permission from the cited references.

Declarations

Competing interests
The authors declare no competing interests.

Received: 1 September 2022 Accepted: 6 April 2023
Published online: 26 April 2023

References

1. Bertok T, Lorencova L, Chocholova E, Jane E, Vikartovska A, Kasak P, et al. Electrochemical Impedance spectroscopy based biosensors: mechanistic principles, analytical examples and challenges towards commercialization for assays of protein cancer biomarkers. Chem Electro Chem. 2019;6:989–1003.
2. Kim WH, Lee JU, Jeon MJ, Park KH, Sim SJ. Three-dimensional hierarchical plasmonic nano-architecture based label-free surface-enhanced Raman spectroscopy detection of urinary exosomal miRNA for clinical diagnosis of prostate cancer. Biosens Bioelectron. 2022;205:114116.
3. Velmanickam L, Jayasooriya V, Nawarathna D. Integrated dielectrophoretic and impedimetric biosensor provides a template for universal biomarker sensing in clinical samples. Electrophoresis. 2021;42:1060–9.
4. Gudagunti FD, Gundlakunta SG, Lima IT Jr. Dielectrophoresis-based biosensor for detection of the cancer biomarkers CEA and CA 242 in serum. Chemosensors. 2022;10:104.
5. Denoroy L, Zimmer L, Renaud B, Parrot S. Ultra high performance liquid chromatography as a tool for the discovery and the analysis of biomarkers of diseases: a review. J Chromatogr B. 2013;927:37–53.
6. Wang X, Li H, Zou X, Yan X, Cong P, Li H, et al. Deep mining and quantification of oxidized cholesteryl esters discovers potential biomarkers involved in breast cancer by liquid chromatography-mass spectrometry. J Chromatogr A. 2022;1663:462764.
7. Jayanthi VSA, Das AB, Saxena U. Recent advances in biosensor development for the detection of cancer biomarkers. Biosens Bioelectron. 2017;91:15–23.
8. Kaya SI, Ozcelikay G, Mollarasouli F, Bakirhan NK, Ozkan SA. Recent achievements and challenges on nanomaterial based electrochemical biosensors for the detection of colon and lung cancer biomarkers. Sens Actuators B. 2022;351:130856.
9. Sharifi M, Hasan A, Attar F, Taghizadeh A, Falahati M. Development of point-of-care nanobiosensors for breast cancers diagnosis. Talanta. 2020;217:121091.
10. Vendrell M, Maiti KK, Dhaliwal K, Chang YT. Surface-enhanced Raman scattering in cancer detection and imaging. Trends Biotechnol. 2013;31(4):249–57.
11. Guerrini L, Garcia-Rico E, O'Loghlen A, Giannini V, Alvarez-Puebla RA. Surface-enhanced Raman scattering (SERS) spectroscopy for sensing and characterization of exosomes in cancer diagnosis. Cancers. 2021;13:2179.
12. Elkady A, Hassan M, Hagag MF, El-Ahwany E, Helal OM, Zoheiry M, Abdalla MA, Elzallat M. Innovative model of surface-enhanced Raman spectroscopy for exosomes identification: An approach for the diagnosis of hepatocellular carcinoma. Clinica Chimica Acta. 2023 Jan 13:117228.
13. Chen C, Liu W, Tian S, Hong T. Novel surface-enhanced Raman spectroscopy techniques for DNA, protein and drug detection. Sensors. 2019;19:1712.
14. Kondo T. Cancer biomarker development and two-dimensional difference gel electrophoresis (2D-DIGE). Biochimica et Biophysica Acta (BBA)-Proteins and Proteomics. 2019; 1867: 2–8.
15. Van den Broek I, Sparidans RW, Schellens JH, Beijnen JH. Quantitative assay for six potential breast cancer biomarker peptides in human serum by liquid chromatography coupled to tandem mass spectrometry. J Chromatogr B. 2010;878:590–602.
16. Lee GB, Lee JC, Moon MH. Plasma lipid profile comparison of five different cancers by nanoflow ultrahigh performance liquid chromatography-tandem mass spectrometry. Anal Chim Acta. 2019;1063:117–26.
17. Zhang F, Deng CK, Wang M, Deng B, Barber R, Huang G. Identification of novel alternative splicing biomarkers for breast cancer with LC/MS/MS and RNA-Seq. BMC Bioinformatics. 2020;21:1–17.
18. Godoy AT, Eberlin MN, Simionato AVC. Targeted metabolomics: liquid chromatography coupled to mass spectrometry method development and validation for the identification and quantitation of modified nucleosides as putative cancer biomarkers. Talanta. 2020;210:120640.
19. Sharifi M, Hosseinali SH, Alizadeh RH, Hasan A, Attar F, Salihi A, et al. Plasmonic and chiroplasmonic nanobiosensors based on gold nanoparticles. Talanta. 2020;212:120782.
20. Khan S, Hasan A, Attar F, Babadaei MMN, Zeinabad HA, Salehi M, et al. Diagnostic and drug release systems based on microneedle arrays in breast cancer therapy. J Controlled Release. 2021;338:341–57.
21. Emami M, Shamsipur M, Saber R, Irajirad R. An electrochemical immunosensor for detection of a breast cancer biomarker based on antiHER2–iron oxide nanoparticle bioconjugates. Analyst. 2014;139:2858–66.
22. Feng D, Li L, Zhao J, Zhang Y. Simultaneous electrochemical detection of multiple biomarkers using gold nanoparticles decorated multiwall carbon nanotubes as signal enhancers. Anal Biochem. 2015;482:48–54.
23. Salahandish R, Ghaffarinejad A, Omidinia E, Zargartalebi H, Majidzadeh-A K, Naghib SM, et al. Label-free ultrasensitive detection of breast cancer miRNA-21 biomarker employing electrochemical nano-genosensor based on sandwiched AgNPs in PANI and N-doped graphene. Biosens Bioelectron. 2018;120:129–36.
24. Pothipor C, Jakmunee J, Bamrungsap S, Ounnunkad K. An electrochemical biosensor for simultaneous detection of breast cancer clinically related microRNAs based on a gold nanoparticles/graphene quantum dots/graphene oxide film. Analyst. 2021;146:4000–9.
25. Yan R, Lu N, Han S, Lu Z, Xiao Y, Zhao Z, et al. Simultaneous detection of dual biomarkers using hierarchical MoS2 nanostructuring and nano-signal amplification-based electrochemical aptasensor toward accurate diagnosis of prostate cancer. Biosens Bioelectron. 2022;197:113797.
26. Hassan MH, Vyas C, Grieve B, Bartolo P. Recent advances in enzymatic and non-enzymatic electrochemical glucose sensing. Sensors. 2021;21:4672.
27. Sharifi M, Hosseinali SH, Yousefvand P, Salihi A, Shekha MS, Aziz FM, et al. Gold nanozyme: biosensing and therapeutic activities. Mater Sci Engineering: C. 2020;108:110422.
28. Khan S, Babadaei MMN, Hasan A, Edis Z, Attar F, Siddique R, et al. Enzyme–polymeric/inorganic metal oxide/hybrid nanoparticle bio-conjugates in the development of therapeutic and biosensing platforms. J Adv Res. 2021;33:227–39.
29. Tomic E. Thermal stability of coordination polymers. J Appl Polym Sci. 1965;9:3745–52.
30. Yaghi OM, Li G, Li H. Selective binding and removal of guests in a microporous metal–organic framework. Nature. 1995;378:703–6.

31. Sindoro M, Yanai N, Jee A-Y, Granick S. Colloidal-sized metal–organic frameworks: synthesis and applications. Acc Chem Res. 2014;47:459–69.
32. Cai G, Yan P, Zhang L, Zhou H-C, Jiang H-L. Metal–organic framework-based hierarchically porous materials: synthesis and applications. Chem Rev. 2021;121:12278–326.
33. Zhou Y, Abazari R, Chen J, Tahir M, Kumar A, Ikreedeegh RR, et al. Bimetallic metal–organic frameworks and MOF-derived composites: recent progress on electro-and photoelectrocatalytic applications. Coord Chem Rev. 2022;451:214264.
34. Zhao Z, Ding J, Zhu R, Pang H. The synthesis and electrochemical applications of core–shell MOFs and their derivatives. J Mater Chem A. 2019;7:15519–40.
35. Wu X-Q, Liu Y, Feng P-Q, Wei X-H, Yang G-M, Qiu X-H, et al. Design of a Zn-MOF biosensor via a ligand "lock" for the recognition and distinction of S-containing amino acids. Chem Commun. 2019;55:4059–62.
36. Sarabaegi M, Roushani M, Hosseini H, Saedi Z, Lemraski EG. A novel ultrasensitive biosensor based on NiCo-MOF nanostructure and confined to flexible carbon nanofibers with high-surface skeleton to rapidly detect Helicobacter pylori. Mater Sci Semiconduct Process. 2022;139:106351.
37. Rosen AS, Notestein JM, Snurr RQ. Realizing the data-driven, computational discovery of metal-organic framework catalysts. Curr Opin Chem Eng. 2022;35:100760.
38. Liu J, Goetjen TA, Wang Q, Knapp JG, Wasson MC, Yang Y, et al. MOF-enabled confinement and related effects for chemical catalyst presentation and utilization. Chem Soc Rev. 2022;51:1045.
39. Zeraati M, Alizadeh V, Kazemzadeh P, Safinejad M, Kazemian H, Sargazi G. A new nickel metal organic framework (Ni-MOF) porous nanostructure as a potential novel electrochemical sensor for detecting glucose. J Porous Mater. 2022;29:257–67.
40. Mu Z, Tian J, Wang J, Zhou J, Bai L. A new electrochemical aptasensor for ultrasensitive detection of endotoxin using Fe-MOF and AgNPs decorated PN-CNTs as signal enhanced indicator. Appl Surf Sci. 2022;573:151601.
41. Dang S, Zhu Q-L, Xu Q. Nanomaterials derived from metal–organic frameworks. Nat Reviews Mater. 2017;3:1–14.
42. Arbulu RC, Jiang YB, Peterson EJ, Qin Y. Metal–organic framework (MOF) nanorods, nanotubes, and nanowires. Angew Chem Int Ed. 2018;57:5813–7.
43. Dai S, Tissot A, Serre C. Recent Progresses in Metal–Organic Frameworks Based Core–shell Composites.Advanced Energy Materials. 2021:2100061.
44. Chen L, Luque R, Li Y. Controllable design of tunable nanostructures inside metal–organic frameworks. Chemical Society Reviews. 2017;46:4614–30.
45. Berijani K, Morsali A. The role of metal–organic porous frameworks in dual catalysis.Inorganic Chemistry Frontiers. 2021.
46. Zeng Y, Xu G, Kong X, Ye G, Guo J, Lu C, Nezamzadeh-Ejhieh A, Khan MS, Liu J, Peng Y. Recent advances of the core-shell MOFs in tumour therapy. Int J Pharm. 2022 ; 24:122228.
47. Wu B, Fu J, Zhou Y, Luo S, Zhao Y, Quan G, et al. Tailored core–shell dual metal–organic frameworks as a versatile nanomotor for effective synergistic antitumor therapy. Acta Pharm Sinica B. 2020;10:2198–211.
48. Zhang H-W, Zhu Q-Q, Yuan R, He H. Crystal engineering of MOF@ COF core-shell composites for ultra-sensitively electrochemical detection. Sens Actuators B. 2021;329:129144.
49. He L, Liu Y, Liu J, Xiong Y, Zheng J, Liu Y, et al. Core–shell noble-metal@ metal-organic-framework nanoparticles with highly selective sensing property. Angew Chem. 2013;125:3829–33.
50. Hong DH, Shim HS, Ha J, Moon HR. MOF-on-MOF Architectures: applications in separation, catalysis, and sensing. Bull Korean Chem Soc. 2021;42:956–69.
51. Tang J, Tang D. Non-enzymatic electrochemical immunoassay using noble metal nanoparticles: a review. Microchim Acta. 2015;182:2077–89.
52. Hong F, Wang Q, Wang W, Chen X, Cao Y, Dong Y, et al. Background signal-free and highly sensitive electrochemical aptasensor for rapid detecting tumor markers with Pb-MOF functionalized dendritic DNA probes. J Electroanal Chem. 2020;861:113956.
53. Srivastava M, Nirala NR, Srivastava S, Prakash R. A comparative study of aptasensor vs immunosensor for label-free PSA cancer detection on GQDs-AuNRs modified screen-printed electrodes. Sci Rep. 2018;8:1–11.
54. Malecka K, Mikuła E, Ferapontova EE. Design strategies for electrochemical aptasensors for cancer diagnostic devices. Sensors. 2021;21:736.
55. Omage JI, Easterday E, Rumph JT, Brula I, Hill B, Kristensen J, et al. Cancer Diagnostics and early detection using Electrochemical Aptasensors. Micromachines. 2022;13:522.
56. He L, Huang R, Xiao P, Liu Y, Jin L, Liu H, et al. Current signal amplification strategies in aptamer-based electrochemical biosensor: a review. Chin Chem Lett. 2021;32:1593–602.
57. Yuan M, Qian S, Cao H, Yu J, Ye T, Wu X, et al. An Ultra-sensitive electrochemical aptasensor for simultaneous quantitative detection of Pb2 + and Cd2 + in fruit and vegetable. Food Chem. 2022;382
58. Jiang H, Sun Z, Zhang C, Weng X. 3D-architectured aptasensor for ultrasensitive electrochemical detection of norovirus based on phosphorene-gold nanocomposites. Sens Actuators B. 2022;354:131232.
59. Xu R, Abune L, Davis B, Ouyang L, Zhang G, Wang Y, et al. Ultrasensitive detection of small biomolecules using aptamer-based molecular recognition and nanoparticle counting. Biosens Bioelectron. 2022;203.
60. Zhou N, Su F, Guo C, He L, Jia Z, Wang M, et al. Two-dimensional oriented growth of Zn-MOF-on-Zr-MOF architecture: a highly sensitive and selective platform for detecting cancer markers. Biosens Bioelectron. 2019;123:51–8.
61. Stock N, Biswas S. Synthesis of metal-organic frameworks (MOFs): routes to various MOF topologies, morphologies, and composites. Chem Rev. 2012;112:933–69.
62. Abednatanzi S, Derakhshandeh PG, Depauw H, Coudert F-X, Vrielinck H, Van Der Voort P, et al. Mixed-metal metal–organic frameworks. Chem Soc Rev. 2019;48:2535–65.
63. Yang J, Ye H, Zhao F, Zeng B. A novel Cu x O nanoparticles@ ZIF-8 composite derived from core–shell metal–organic frameworks for highly selective electrochemical sensing of hydrogen peroxide. ACS Appl Mater Interfaces. 2016;8:20407–14.
64. Luo J, Cui J, Wang Y, Yu D, Qin Y, Zheng H, et al. MOF-derived porous CeO 2 – x/C nanorods and their applications in uric acid biosensor. NANO. 2018;13:1850085.
65. Wang Z, Dong P, Sun Z, Sun C, Bu H, Han J, et al. NH 2-Ni-MOF electrocatalysts with tunable size/morphology for ultrasensitive C-reactive protein detection via an aptamer binding induced DNA walker–antibody sandwich assay. J Mater Chem B. 2018;6:2426–31.
66. Lopa NS, Rahman MM, Ahmed F, Ryu T, Lei J, Choi I, et al. A chemically and electrochemically stable, redox-active and highly sensitive metal azolate framework for non-enzymatic electrochemical detection of glucose. J Electroanal Chem. 2019;840:263–71.
67. Lopa NS, Rahman MM, Ahmed F, Sutradhar SC, Ryu T, Kim W. A Ni-based redox-active metal-organic framework for sensitive and non-enzymatic detection of glucose. J Electroanal Chem. 2018;822:43–9.
68. Yang M, Sun Z, Jin H, Gui R. Urate oxidase-loaded MOF electrodeposited on boron nanosheet-doxorubicin complex as multifunctional nano-enzyme platform for enzymatic and ratiometric electrochemical biosensing. Talanta. 2022;243:123359.
69. Wang Z, Gui M, Asif M, Yu Y, Dong S, Wang H, et al. A facile modular approach to the 2D oriented assembly MOF electrode for non-enzymatic sweat biosensors. Nanoscale. 2018;10:6629–38.
70. Wang Z, Liu T, Yu Y, Asif M, Xu N, Xiao F, et al. Coffee ring–inspired approach toward oriented self-assembly of biomimetic murray MOFs as sweat biosensor. Small. 2018;14:1802670.
71. Bai W, Li S, Ma J, Cao W, Zheng J. Ultrathin 2D metal–organic framework (nanosheets and nanofilms)-based x D–2D hybrid nanostructures as biomimetic enzymes and supercapacitors. J Mater Chem A. 2019;7:9086–98.
72. Huang W, Xu Y, Wang Z, Liao K, Zhang Y, Sun Y. Dual nanozyme based on ultrathin 2D conductive MOF nanosheets intergraded with gold nanoparticles for electrochemical biosensing of H2O2 in cancer cells. Talanta. 2022;249:123612.
73. Chen S, Xie Y, Guo X, Sun D. Self-supporting electrochemical sensors for monitoring of cell-released H2O2 based on metal nanoparticle/MOF nanozymes. Microchem J. 2022;181:107715.

74. Chen D, Sun D, Wang Z, Qin W, Chen L, Zhou L, et al. A DNA nanostructured aptasensor for the sensitive electrochemical detection of HepG2 cells based on multibranched hybridization chain reaction amplification strategy. Biosens Bioelectron. 2018;117:416–21.
75. Wang H, Jian Y, Kong Q, Liu H, Lan F, Liang L, et al. Ultrasensitive electrochemical paper-based biosensor for microRNA via strand displacement reaction and metal-organic frameworks. Sens Actuators B. 2018;257:561–9.
76. Li W, Chen S, Yang Y, Song Y, Ma C, Qiao X, et al. Ultrasensitive electrochemical immunosensor based on the signal amplification strategy of the competitive reaction of Zn2 + and ATP ions to construct a "signal on" mode GOx-HRP enzyme cascade reaction. Microchim Acta. 2021;188:61.
77. Wan H, Cao X, Liu M, Zhang F, Sun C, Xia J, et al. Aptamer and bifunctional enzyme co-functionalized MOF-derived porous carbon for low-background electrochemical aptasensing. Anal Bioanal Chem. 2021;413:6303–12.
78. Pang Y-H, Guo L-L, Shen X-F, Yang N-C, Yang C. Rolling circle amplified DNAzyme followed with covalent organic frameworks: Cascade signal amplification of electrochemical ELISA for alfatoxin M1 sensing. Electrochim Acta. 2020;341:136055.
79. Ma J, Chen G, Bai W, Zheng J. Amplified electrochemical hydrogen peroxide sensing based on Cu-porphyrin metal–organic framework nanofilm and G-quadruplex-hemin DNAzyme. ACS Appl Mater Interfaces. 2020;12:58105–12.
80. Fu X, He J, Zhang C, Chen J, Wen Y, li J, et al. Trimetallic signal amplification aptasensor for TSP-1 detection based on Ce-MOF@Au and AuPtRu nanocomposites. Biosens Bioelectron. 2019;132:302–9.
81. Li J, Liu L, Ai Y, Liu Y, Sun H, Liang Q. Self-polymerized dopamine-decorated au NPs and coordinated with Fe-MOF as a dual binding sites and dual signal-amplifying electrochemical aptasensor for the detection of CEA. ACS Appl Mater Interfaces. 2020;12:5500–10.
82. Guo L, Mu Z, Yan B, Wang J, Zhou J, Bai L. A novel electrochemical biosensor for sensitive detection of non-small cell lung cancer ctDNA using NG-PEI-COFTAPB-TFPB as sensing platform and Fe-MOF for signal enhancement. Sens Actuators B. 2022;350:130874.
83. Hatami Z, Jalali F, Amouzadeh Tabrizi M, Shamsipur M. Application of metal-organic framework as redox probe in an electrochemical aptasensor for sensitive detection of MUC1. Biosens Bioelectron. 2019;141:111433.
84. Liu F, Geng L, Ye F, Zhao S. MOF-derivated MnO@C nanocomposite with bidirectional electrocatalytic ability as signal amplification for dual-signal electrochemical sensing of cancer biomarker. Talanta. 2022;239:123150.
85. Sun Y, Jin H, Jiang X, Gui R. Assembly of black phosphorus nanosheets and MOF to form functional hybrid thin-film for precise protein capture, dual-signal and intrinsic self-calibration sensing of specific cancer-derived exosomes. Anal Chem. 2020;92:2866–75.
86. Feng J, Wang H, Ma Z. Ultrasensitive amperometric immunosensor for the prostate specific antigen by exploiting a Fenton reaction induced by a metal-organic framework nanocomposite of type Au/Fe-MOF with peroxidase mimicking activity. Microchim Acta. 2020;187:95.
87. Yola ML. Sensitive sandwich-type voltammetric immunosensor for breast cancer biomarker HER2 detection based on gold nanoparticles decorated Cu-MOF and Cu2ZnSnS4 NPs/Pt/g-C3N4 composite. Microchim Acta. 2021;188:78.
88. Ou D, Sun D, Liang Z, Chen B, Lin X, Chen Z. A novel cytosensor for capture, detection and release of breast cancer cells based on metal organic framework PCN-224 and DNA tetrahedron linked dual-aptamer. Sens Actuators B. 2019;285:398–404.
89. Ehzari H, Samimi M, Safari M, Gholivand MB. Label-free electrochemical immunosensor for sensitive HER2 biomarker detection using the core-shell magnetic metal-organic frameworks. J Electroanal Chem. 2020;877:114722.
90. Bhardwaj SK, Sharma AL, Bhardwaj N, Kukkar M, Gill AAS, Kim K-H, et al. TCNQ-doped Cu-metal organic framework as a novel conductometric immunosensing platform for the quantification of prostate cancer antigen. Sens Actuators B. 2017;240:10–7.
91. Guo C, Su F, Song Y, Hu B, Wang M, He L, et al. Aptamer-templated silver nanoclusters embedded in zirconium metal–organic framework for bifunctional electrochemical and SPR aptasensors toward carcinoembryonic antigen. ACS Appl Mater Interfaces. 2017;9:41188–99.
92. Duan F, Hu M, Guo C, Song Y, Wang M, He L, et al. Chromium-based metal-organic framework embedded with cobalt phthalocyanine for the sensitively impedimetric cytosensing of colorectal cancer (CT26) cells and cell imaging. Chem Eng J. 2020;398:125452.
93. Li Y, Hu M, Huang X, Wang M, He L, Song Y, et al. Multicomponent zirconium-based metal-organic frameworks for impedimetric aptasensing of living cancer cells. Sens Actuators B. 2020;306:127608.
94. Cao JT, Wang YL, Zhang JJ, Zhou YJ, Ren SW, Liu YM. Efficient electrochemiluminescence quenching of carbon-coated petalous CdS nanoparticles for an ultrasensitive tumor marker assay through coreactant consumption by G-quadruplex-hemin decorated au nanorods. RSC Adv. 2016;6:86682–7.
95. Huang W, Hu G-B, Yao L-Y, Yang Y, Liang W-B, Yuan R, et al. Matrix coordination-induced electrochemiluminescence enhancement of tetraphenylethylene-based hafnium metal–organic framework: an electrochemiluminescence chromophore for ultrasensitive electrochemiluminescence sensor construction. Anal Chem. 2020;92:3380–7.
96. Wang J-M, Yao L-Y, Huang W, Yang Y, Liang W-B, Yuan R, et al. Overcoming aggregation-induced quenching by metal – organic framework for electrochemiluminescence (ECL) enhancement: Zn-PTC as a new ECL emitter for ultrasensitive MicroRNAs detection. ACS Appl Mater Interfaces. 2021;13:44079–85.
97. Zhong Y, Wang X, Zha R, Wang C, Zhang H, Wang Y, et al. Dual-wavelength responsive photoelectrochemical aptasensor based on ionic liquid functionalized Zn-MOFs and noble metal nanoparticles for the simultaneous detection of multiple tumor markers. Nanoscale. 2021;13:19066–75.
98. Wu Y, Chen X, Luo X, Yang M, Hou C, Huo D. Bimetallic organic framework Cu/UiO-66 mediated "fluorescence turn-on" method for ultrasensitive and rapid detection of carcinoembryonic antigen (CEA). Anal Chim Acta. 2021;1183:339000.
99. Zhou X, Zhu Q, Yang Y. Aptamer-integrated nucleic acid circuits for biosensing: classification, challenges and perspectives. Biosens Bioelectron. 2020;165:112422.
100. Shaban SM, Kim D-H. Recent advances in aptamer sensors. Sensors. 2021;21:979.
101. Roy D, Pascher A, Juratli MA, Sporn JC. The potential of aptamer-mediated liquid biopsy for early detection of cancer. Int J Mol Sci. 2021;22:5601.
102. Han J, Gao L, Wang J, Wang J. Application and development of aptamer in cancer: from clinical diagnosis to cancer therapy. J Cancer. 2020;11:6902.
103. Jo H, Ban C. Aptamer–nanoparticle complexes as powerful diagnostic and therapeutic tools. Exp Mol Med. 2016;48:e230–e.
104. Ilgu M, Nilsen-Hamilton M. Aptamers in analytics. Analyst. 2016;141:1551–68.
105. Kim M, Kim D-M, Kim K-S, Jung W, Kim D-E. Applications of cancer cell-specific aptamers in targeted delivery of anticancer therapeutic agents. Molecules. 2018;23:830.
106. Morita Y, Leslie M, Kameyama H, Volk DE, Tanaka T. Aptamer therapeutics in cancer: current and future. Cancers. 2018;10:80.
107. Pereira RL, Nascimento IC, Santos AP, Ogusuku IE, Lameu C, Mayer G, et al. Aptamers: novelty tools for cancer biology. Oncotarget. 2018;9:26934.
108. Coker-Gurkan A, Obakan-Yerlikaya P, Arisan E-D. Applications of aptamers in cancer therapy.Cancer Manag Ther. 2018.
109. Elaiwi FA, Sirkecioglu A. Amine-functionalized metal organic frameworks MIL-101 (cr) adsorbent for copper and cadmium ions in single and binary solution. Sep Sci Technol. 2020;55:3362–74.
110. Jeyaseelan A, Naushad M, Ahamad T, Viswanathan N. Design and development of amine functionalized iron based metal organic frameworks for selective fluoride removal from water environment. J Environ Chem Eng. 2021;9:104563.
111. Sharifzadeh Z, Morsali A. Amine-Functionalized Metal-Organic Frameworks: from Synthetic Design to Scrutiny in Application. Coord Chem Rev. 2022;459:214445.
112. Kahn JS, Freage L, Enkin N, Garcia MAA, Willner I. Stimuli-Responsive DNA-Functionalized Metal–Organic Frameworks (MOFs). Adv Mater. 2017;29:1602782.

113. Chen Y, Chen W, Tian Y, Zhu P, Liu S, Du L, et al. DNA and RhoB-functionalized metal–organic frameworks for the sensitive fluorescent detection of liquid alcohols. Microchem J. 2021;170:106688.
114. Morris W, Briley WE, Auyeung E, Cabezas MD, Mirkin CA. Nucleic acid–metal organic framework (MOF) nanoparticle conjugates. J Am Chem Soc. 2014;136:7261–4.
115. Cui L, Wu J, Li J, Ju H. Electrochemical sensor for lead cation sensitized with a DNA functionalized porphyrinic metal–organic framework. Anal Chem. 2015;87:10635–41.
116. Mejia-Ariza R, Rosselli J, Breukers C, Manicardi A, Terstappen LW, Corradini R, et al. DNA detection by Flow Cytometry using PNA-Modified Metal–Organic Framework particles. Chemistry–A Eur J. 2017;23:4180–6.
117. Ning W, Di Z, Yu Y, Zeng P, Di C, Chen D, et al. Imparting designer biorecognition functionality to metal–organic frameworks by a DNA-mediated surface engineering strategy. Small. 2018;14:1703812.
118. Wu LL, Wang Z, Zhao SN, Meng X, Song XZ, Feng J, et al. A metal–organic framework/DNA hybrid system as a novel fluorescent biosensor for mercury (II) ion detection. Chemistry–A Eur J. 2016;22:477–80.
119. Vázquez-González M, Willner I. DNA-responsive SiO2 nanoparticles, metal–organic frameworks, and microcapsules for controlled drug release. Langmuir. 2018;34:14692–710.
120. Lv M, Zhou W, Tavakoli H, Bautista C, Xia J, Wang Z, et al. Aptamer-functionalized metal-organic frameworks (MOFs) for biosensing. Biosens Bioelectron. 2021;176:112947.
121. Liu B, Jiang M, Zhu D, Zhang J, Wei G. Metal-organic frameworks functionalized with nucleic acids and amino acids for structure- and function-specific applications: a tutorial review. Chem Eng J. 2022;428:131118.
122. Hansen JA, Wang J, Kawde A-N, Xiang Y, Gothelf KV, Collins G. Quantum-dot/aptamer-based ultrasensitive multi-analyte electrochemical biosensor. J Am Chem Soc. 2006;128:2228–9.
123. Rhouati A, Marty J-L, Vasilescu A. Metal nanomaterial-assisted aptasensors for emerging pollutants detection. Nanotechnol Biosens. 2018. https://doi.org/10.1016/B978-0-12-813855-7.00007-6.
124. Zhu Y, Chandra P, Shim Y-B. Ultrasensitive and selective electrochemical diagnosis of breast cancer based on a hydrazine–Au nanoparticle–aptamer bioconjugate. Anal Chem. 2013;85:1058–64.
125. Mahmoudpour M, Karimzadeh Z, Ebrahimi G, Hasanzadeh M, Dolatabadi Ezzati Nazhad, J. Synergizing functional nanomaterials with aptamers based on electrochemical strategies for pesticide detection: current status and perspectives. Critic Rev Anal Chem. 2021;52:1–28.
126. Zhang Z, Ji H, Song Y, Zhang S, Wang M, Jia C, et al. Fe (III)-based metal–organic framework-derived core–shell nanostructure: sensitive electrochemical platform for high trace determination of heavy metal ions. Biosens Bioelectron. 2017;94:358–64.
127. He L, Duan F, Song Y, Guo C, Zhao H, Tian J-Y, et al. 2D zirconium-based metal-organic framework nanosheets for highly sensitive detection of mucin 1: consistency between electrochemical and surface plasmon resonance methods. 2D Mater. 2017;4:025098.
128. Xie Q, Xu Z, Huang G, Lin C, Lin X. Bioinspired polydopamine-mediated metal-organic framework click-grafting aptamers functionalized fabric for highly-specific recognition of microcystin-leucine arginine. Journal of Chromatography A. 2023 Jan 11;1688:463728.
129. Zheng Y, Sun FZ, Han X, Xu J, Bu XH. Recent progress in 2D metal-organic frameworks for optical applications. Adv Opt Mater. 2020;8:2000110.
130. Han R, Sun Y, Lin Y, Liu H, Dai Y, Zhu X, et al. A simple chemiluminescent aptasensor for the detection of α-fetoprotein based on iron-based metal organic frameworks. New J Chem. 2020;44:4099–107.
131. Mohan B, Kumar S, Xi H, Ma S, Tao Z, Xing T, et al. Fabricated metal-organic frameworks (MOFs) as luminescent and electrochemical biosensors for cancer biomarkers detection. Biosens Bioelectron. 2022;197:113738.
132. Du X, Fu W, Su P, Cai J, Zhou M. Internal-micro-electrolysis-enhanced heterogeneous electro-Fenton process catalyzed by Fe/Fe3C@ PC core–shell hybrid for sulfamethazine degradation. Chem Eng J. 2020;398:125681.
133. Ye Z, Padilla JA, Xuriguera E, Beltran JL, Alcaide F, Brillas E, et al. A highly stable metal–organic framework-engineered FeS2/C nanocatalyst for heterogeneous electro-Fenton treatment: validation in wastewater at mild pH. Environ Sci Technol. 2020;54:4664–74.
134. Yao Y, Wang C, Na J, Hossain MSA, Yan X, Zhang H, et al. Macroscopic MOF architectures: effective strategies for practical application in water treatment. Small. 2022;18:2104387.
135. Qu B, Chu X, Shen G, Yu R. A novel electrochemical immunosensor based on colabeled silica nanoparticles for determination of total prostate specific antigen in human serum. Talanta. 2008;76:785–90.
136. Wan Y, Deng W, Su Y, Zhu X, Peng C, Hu H, et al. Carbon nanotube-based ultrasensitive multiplexing electrochemical immunosensor for cancer biomarkers. Biosens Bioelectron. 2011;30:93–9.
137. Xu S, Liu Y, Wang T, Li J. Positive potential operation of a cathodic electrogenerated chemiluminescence immunosensor based on luminol and graphene for cancer biomarker detection. Anal Chem. 2011;83:3817–23.
138. Mao K, Wu D, Li Y, Ma H, Ni Z, Yu H, et al. Label-free electrochemical immunosensor based on graphene/methylene blue nanocomposite. Anal Biochem. 2012;422:22–7.
139. Lee J, Dak P, Lee Y, Park H, Choi W, Alam MA, et al. Two-dimensional layered MoS2 biosensors enable highly sensitive detection of biomolecules. Sci Rep. 2014;4:1–7.
140. Jang HD, Kim SK, Chang H, Choi J-W. 3D label-free prostate specific antigen (PSA) immunosensor based on graphene–gold composites. Biosens Bioelectron. 2015;63:546–51.
141. Pei H, Zhu S, Yang M, Kong R, Zheng Y, Qu F. Graphene oxide quantum dots@ silver core–shell nanocrystals as turn-on fluorescent nanoprobe for ultrasensitive detection of prostate specific antigen. Biosens Bioelectron. 2015;74:909–14.
142. Xu Y, Wang X, Ding C, Luo X. Ratiometric antifouling electrochemical biosensors based on multifunctional peptides and MXene loaded with au nanoparticles and methylene blue. ACS Appl Mater Interfaces. 2021;13:20388–96.
143. Feng D, Su J, Xu Y, He G, Wang C, Wang X, et al. DNA tetrahedron-mediated immune-sandwich assay for rapid and sensitive detection of PSA through a microfluidic electrochemical detection system. Microsyst Nanoeng. 2021;7:1–10.
144. Pourmadadi M, Nouralishahi A, Shalbaf M, Shabani Shayeh J, Nouralishahi A. An electrochemical aptasensor for detection of prostate-specific antigen-based on carbon quantum dots-gold nanoparticles. Biotechnol Appl Biochem. 2022;70:175.
145. Xu X. Sensitive electrochemiluminescence immunosensor for determination of tumor biomarker PSA based on multifunctionalized Pt/Ag@ BSA core-shell nanoparticles. Bull Korean Chem Soc. 2016;37(4):452–7.
146. Li M, Wang P, Li F, Chu Q, Li Y, Dong Y. An ultrasensitive sandwich-type electrochemical immunosensor based on the signal amplification strategy of mesoporous core–shell Pd@ pt nanoparticles/amino group functionalized graphene nanocomposite. Biosens Bioelectron. 2017;87:752–9.
147. Shao K, Wang B, Nie A, Ye S, Ma J, Li Z, et al. Target-triggered signal-on ratiometric electrochemiluminescence sensing of PSA based on MOF/Au/G-quadruplex. Biosens Bioelectron. 2018;118:160–6.
148. Dai L, Li Y, Wang Y, Luo X, Wei D, Feng R, et al. A prostate-specific antigen electrochemical immunosensor based on pd NPs functionalized electroactive Co-MOF signal amplification strategy. Biosens Bioelectron. 2019;132:97–104.
149. Zhou C, Cui K, Liu Y, Hao S, Zhang L, Ge S, et al. Ultrasensitive microfluidic paper-based electrochemical/visual analytical device via signal amplification of Pd@ hollow Zn/Co Core–Shell ZIF67/ZIF8 nanoparticles for prostate-specific antigen detection. Anal Chem. 2021;93:5459–67.
150. Xiong X, Zhang Y, Wang Y, Sha H, Jia N. One-step electrochemiluminescence immunoassay for breast cancer biomarker CA 15 – 3 based on Ru (bpy) 62+-coated UiO-66-NH2 metal-organic framework. Sens Actuators B. 2019;297:126812.
151. Zhang C, Zhang D, Ma Z, Han H. Cascade catalysis-initiated radical polymerization amplified impedimetric immunosensor for ultrasensitive detection of carbohydrate antigen 15 – 3. Biosens Bioelectron. 2019;137:1–7.
152. Zhou X, Guo S, Gao J, Zhao J, Xue S, Xu W. Glucose oxidase-initiated cascade catalysis for sensitive impedimetric aptasensor based on metal-organic frameworks functionalized with pt nanoparticles and

hemin/G-quadruplex as mimicking peroxidases. Biosens Bioelectron. 2017;98:83–90.
153. Bao T, Fu R, Wen W, Zhang X, Wang S. Target-driven cascade-amplified release of loads from DNA-gated metal–organic frameworks for electrochemical detection of cancer biomarker. ACS Appl Mater Interfaces. 2019;12:2087–94.
154. Wei X-h, Qiao X, Fan J, Hao Y-q, Zhang Y-t, Zhou Y-l, et al. A label-free ECL aptasensor for sensitive detection of carcinoembryonic antigen based on CdS QDs@ MOF and TEOA@ au as bi-coreactants of Ru (bpy) 32+. Microchem J. 2022;173:106910.
155. Gu C, Guo C, Li Z, Wang M, Zhou N, He L, et al. Bimetallic ZrHf-based metal-organic framework embedded with carbon dots: ultra-sensitive platform for early diagnosis of HER2 and HER2-overexpressed living cancer cells. Biosens Bioelectron. 2019;134:8–15.
156. Ravalli A, da Rocha CG, Yamanaka H, Marrazza G. A label-free electrochemical affisensor for cancer marker detection: the case of HER2. Bioelectrochemistry. 2015;106:268–75.
157. Tian S, Zeng K, Yang A, Wang Q, Yang M. A copper based enzyme-free fluorescence ELISA for HER2 detection. J Immunol Methods. 2017;451:78–82.
158. Shen C, Liu S, Li X, Zhao D, Yang M. Immunoelectrochemical detection of the human epidermal growth factor receptor 2 (HER2) via gold nanoparticle-based rolling circle amplification. Microchim Acta. 2018;185:1–8.
159. Yang S, You M, Zhang F, Wang Q, He P. A sensitive electrochemical aptasensing platform based on exonuclease recycling amplification and host-guest recognition for detection of breast cancer biomarker HER2. Sens Actuators B. 2018;258:796–802.
160. Li X, Shen C, Yang M, Rasooly A. Polycytosine DNA electric-current-generated immunosensor for electrochemical detection of human epidermal growth factor receptor 2 (HER2). Anal Chem. 2018;90:4764–9.
161. Arya SK, Zhurauski P, Jolly P, Batistuti MR, Mulato M, Estrela P. Capacitive aptasensor based on interdigitated electrode for breast cancer detection in undiluted human serum. Biosens Bioelectron. 2018;102:106–12.
162. Shamsipur M, Emami M, Farzin L, Saber R. A sandwich-type electrochemical immunosensor based on in situ silver deposition for determination of serum level of HER2 in breast cancer patients. Biosens Bioelectron. 2018;103:54–61.
163. Centane S, Nyokong T. Aptamer versus antibody as probes for the impedimetric biosensor for human epidermal growth factor receptor. J Inorg Biochem. 2022;230:111764.
164. Sharma S, Zapatero-Rodríguez J, Saxena R, O'Kennedy R, Srivastava S. Ultrasensitive direct impedimetric immunosensor for detection of serum HER2. Biosens Bioelectron. 2018;106:78–85.
165. Carvajal S, Fera SN, Jones AL, Baldo TA, Mosa IM, Rusling JF, et al. Disposable inkjet-printed electrochemical platform for detection of clinically relevant HER-2 breast cancer biomarker. Biosens Bioelectron. 2018;104:158–62.
166. Freitas M, Nouws HP, Delerue-Matos C. Electrochemical sensing platforms for HER2-ECD breast cancer biomarker detection. Electroanalysis. 2019;31:121–8.
167. Ahmad SAA, Zaini MS, Kamarudin MA. An electrochemical sandwich immunosensor for the detection of HER2 using antibody-conjugated PbS quantum dot as a label. J Pharm Biomed Anal. 2019;174:608–17.
168. Freitas M, Neves MM, Nouws HP, Delerue-Matos C. Quantum dots as nanolabels for breast cancer biomarker HER2-ECD analysis in human serum. Talanta. 2020;208:120430.
169. Ali MA, Mondal K, Singh C, Malhotra BD, Sharma A. Anti-epidermal growth factor receptor conjugated mesoporous zinc oxide nanofibers for breast cancer diagnostics. Nanoscale. 2015;7:7234–45.
170. Ali MA, Mondal K, Jiao Y, Oren S, Xu Z, Sharma A, et al. Microfluidic immuno-biochip for detection of breast cancer biomarkers using hierarchical composite of porous graphene and titanium dioxide nanofibers. ACS Appl Mater Interfaces. 2016;8:20570–82.
171. Ren X, Wang H, Wu D, Fan D, Zhang Y, Du B, et al. Ultrasensitive immunoassay for CA125 detection using acid site compound as signal and enhancer. Talanta. 2015;144:535–41.
172. Wang X, Deng W, Shen L, Yan M, Yu J. A 3D electrochemical immunodevice based on an au paper electrode and using au nanoflowers for amplification. New J Chem. 2016;40:2835–42.
173. Gasparotto G, Costa JPC, Costa PI, Zaghete MA, Mazon T. Electrochemical immunosensor based on ZnO nanorods-Au nanoparticles nanohybrids for ovarian cancer antigen CA-125 detection. Mater Sci Engineering: C. 2017;76:1240–7.
174. Gazze A, Ademefun R, Conlan RS, Teixeira SR. Electrochemical impedence spectroscopy enabled CA125 detection; toward early ovarian cancer diagnosis using graphene biosensors. J Interdisciplinary Nanomed. 2018;3:82–8.
175. Rafique S, Tabassum S, Akram R. Sensitive competitive label-free electrochemical immunosensor for primal detection of ovarian cancer. Chem Pap. 2020;74:2591–603.
176. Er OF, Kivrak H, Ozok O, Çelik S, Kivrak A. A novel electrochemical sensor for monitoring ovarian cancer tumor protein CA 125 on benzothiophene derivative based electrodes. J Electroanal Chem. 2022;904:115854.
177. Wang M, Hu M, Li Z, He L, Song Y, Jia Q, et al. Construction of Tb-MOF-on-Fe-MOF conjugate as a novel platform for ultrasensitive detection of carbohydrate antigen 125 and living cancer cells. Biosens Bioelectron. 2019;142:111536.
178. Wang S, Ge L, Yan M, Yu J, Song X, Ge S, et al. 3D microfluidic origami electrochemiluminescence immunodevice for sensitive point-of-care testing of carcinoma antigen 125. Sens Actuators B. 2013;176:1–8.
179. Johari-Ahar M, Rashidi M, Barar J, Aghaie M, Mohammadnejad D, Ramazani A, et al. An ultra-sensitive impedimetric immunosensor for detection of the serum oncomarker CA-125 in ovarian cancer patients. Nanoscale. 2015;7:3768–79.
180. Wu L, Sha Y, Li W, Wang S, Guo Z, Zhou J, et al. One-step preparation of disposable multi-functionalized g-C3N4 based electrochemiluminescence immunosensor for the detection of CA125. Sens Actuators B. 2016;226:62–8.
181. Torati SR, Kasturi KC, Lim B, Kim C. Hierarchical gold nanostructures modified electrode for electrochemical detection of cancer antigen CA125. Sens Actuators B. 2017;243:64–71.
182. Büyüktiryaki S, Say R, Denizli A, Ersöz A. Phosphoserine imprinted nanosensor for detection of Cancer Antigen 125. Talanta. 2017;167:172–80.
183. Pakchin PS, Ghanbari H, Saber R, Omidi Y. Electrochemical immunosensor based on chitosan-gold nanoparticle/carbon nanotube as aï»¿ platform and lactate oxidase as aï»¿ label for detection of CA125 oncomarkerï»¿. Biosens Bioelectron. 2018;122:68–74.
184. Li S, Hu C, Chen C, Zhang J, Bai Y, Tan CS, et al. Molybdenum disulfide supported on metal–organic frameworks as an ultrasensitive layer for the electrochemical detection of the ovarian cancer biomarker CA125. ACS Appl Bio Mater. 2021;4:5494–502.
185. Pachauri N, Dave K, Dinda A, Solanki PR. Cubic CeO 2 implanted reduced graphene oxide-based highly sensitive biosensor for non-invasive oral cancer biomarker detection. J Mater Chem B. 2018;6:3000–12.
186. Yang L, Sun X, Wei D, Ju H, Du Y, Ma H, et al. Aggregation-induced electrochemiluminescence bioconjugates of apoferritin-encapsulated iridium (III) complexes for biosensing application. Anal Chem. 2020;93:1553–60.
187. Yang H, Bao J, Huo D, Zeng Y, Wang X, Samalo M, et al. Au doped polythionine and poly-m-Cresol purple: synthesis and their application in simultaneously electrochemical detection of two lung cancer markers CEA and CYFRA21-1. Talanta. 2021;224:121816.
188. Hu K, Cheng J, Wang K, Zhao Y, Liu Y, Yang H, et al. Sensitive electrochemical immunosensor for CYFRA21-1 detection based on AuNPs@ MoS2@ Ti3C2Tx composites. Talanta. 2022;238:122987.
189. Xu Y, Zheng Y, Ma Z. ZIF-8 silencing shell removed by complexation competition reaction for ultrasensitive electrochemical immunoassay. Sens Actuators B. 2020;307:127647.
190. Wang Y, Li Y, Zhuang X, Tian C, Fu X, Luan F. Ru (bpy) 32 + encapsulated cyclodextrin based metal organic framework with improved biocompatibility for sensitive electrochemiluminescence detection of CYFRA21-1 in cell. Biosens Bioelectron. 2021;190:113371.
191. Zhou L, Yang L, Wang C, Jia H, Xue J, Wei Q, et al. Copper doped terbium metal organic framework as emitter for sensitive electrochemiluminescence detection of CYFRA 21 – 1. Talanta. 2022;238:123047.

192. Kumar S, Sharma JG, Maji S, Malhotra BD. Nanostructured zirconia decorated reduced graphene oxide based efficient biosensing platform for non-invasive oral cancer detection. Biosens Bioelectron. 2016;78:497–504.
193. Zeng Y, Bao J, Zhao Y, Huo D, Chen M, Qi Y, et al. A sandwich-type electrochemical immunoassay for ultrasensitive detection of non-small cell lung cancer biomarker CYFRA21-1. Bioelectrochemistry. 2018;120:183–9.
194. Zeng Y, Bao J, Zhao Y, Huo D, Chen M, Yang M, et al. A sensitive label-free electrochemical immunosensor for detection of cytokeratin 19 fragment antigen 21 – 1 based on 3D graphene with gold nanopaticle modified electrode. Talanta. 2018;178:122–8.
195. Wang Y-M, Wu Z, Liu S-J, Chu X. Structure-switching aptamer triggering hybridization chain reaction on the cell surface for activatable theranostics. Anal Chem. 2015;87:6470–4.
196. Lin S, Gao W, Tian Z, Yang C, Lu L, Mergny J-L, et al. Luminescence switch-on detection of protein tyrosine kinase-7 using a G-quadruplex-selective probe. Chem Sci. 2015;6:4284–90.
197. Miao X, Li Z, Zhu A, Feng Z, Tian J, Peng X. Ultrasensitive electrochemical detection of protein tyrosine kinase-7 by gold nanoparticles and methylene blue assisted signal amplification. Biosens Bioelectron. 2016;83:39–44.
198. Liu Z, Chen W, Han Y, Ouyang J, Chen M, Hu S, et al. A label-free sensitive method for membrane protein detection based on aptamer and AgNCs transfer. Talanta. 2017;175:470–6.
199. Li Y, Liu Z, Lu W, Zhao M, Xiao H, Hu T, et al. A label-free electrochemical aptasensor based on the core–shell Cu-MOF@ TpBD hybrid nanoarchitecture for the sensitive detection of PDGF-BB. Analyst. 2021;146:979–88.
200. Liu L, Zhou Y, Liu S, Xu M. The applications of metal – organic frameworks in electrochemical sensors. ChemElectroChem. 2018;5:6–19.
201. Sharifi M, Avadi MR, Attar F, Dashtestani F, Ghorchian H, Rezayat SM, et al. Cancer diagnosis using nanomaterials based electrochemical nanobiosensors. Biosens Bioelectron. 2019;126:773–84.

Publisher's Note